Contrib Mineral Petrol (2003) 144: 484–505
DOI 10.1007/s00410-002-0413-2

L.A. Coogan · G.J. Banks · K.M. Gillis
C.J. MacLeod · J.A. Pearce

Hidden melting signatures recorded in the Troodos ophiolite plutonic suite: evidence for widespread generation of depleted melts and intra-crustal melt aggregation

Received: 24 April 2002 / Accepted: 4 September 2002 / Published online: 1 November 2002

Abstract The main plutonic complex of the Troodos ophiolite, north of the Arakapas Fault Zone, has been re-examined both from field and geochemical perspectives. Ion microprobe analyses of clinopyroxene crystal cores show that the range of melt compositions added to the lower crust far exceeds that of published lavas in the main Troodos massif. This suggests that the lower crust acted as a filter into which a large range of melt compositions were added and out of which a homogenised (and generally fractionated) derivative was extracted. This crustal-level aggregation homogenised diverse melt fractions from a broad range of degrees of melting. Depleted melts with U-shaped rare earth element (REE) patterns were a significant component of the melts added to the crust, but because of their low incompatible element abundances, mixing with less depleted melts prior to eruption masked their signature in the lavas. The discovery that highly depleted melts constituted a significant component of the melts added to the Troodos crust, but not of the lavas, demonstrates that the spatial distribution of lava-types is not necessarily a good indicator of where different parental melt compositions are generated within the mantle. Compared with normal mid-ocean ridge basalts, the Troodos parental melts were (1) generally depleted in immobile incompatible trace elements, (2) less depleted in light REE (LREE) than would be expected for the concomitant depletion in middle and heavy REE, (3) enriched in Sr with respect to the LREE and (4) more oxidised. Modelling of these characteristics suggests a mantle source that had previously lost a significant melt fraction under relatively reducing conditions. This was followed by remelting under more oxidising conditions in an environment in which Sr and LREE were added to the source consistent with previous models of a supra-subduction zone setting.

L.A. Coogan (✉) · G.J. Banks · C.J. MacLeod · J.A. Pearce
Department of Earth Sciences,
Cardiff University, Cardiff CF10 3YE, UK
E-mail: lac@le.ac.uk
Tel.: +1-44-1162523608
Fax: +1-44-1162523918

K.M. Gillis
School of Earth and Ocean Sciences,
University of Victoria, P.O. Box 3055, Victoria,
British Columbia V8W 3P6, Canada

Present address: L.A. Coogan
Department of Geology,
University of Leicester, University Road,
Leicester, LE1 7RH, UK

Editorial responsibility: T.L. Grove

Introduction

Understanding magma plumbing at oceanic spreading centres requires detailed studies of the entire plumbing system. Early work concentrated on the extrusive portion of the oceanic crust and this was followed by investigations of samples of the upper part of the residual mantle. In more recent years, the role of magma chambers and, thus, the plutonic section of oceanic crust, has been given greater consideration. Studies of the lower oceanic crust allow us to investigate the compositional diversity of melts feeding the crust and how these are mixed and fractionated prior to eruption. In turn, this allows a greater understanding of the processes of mantle melting and melt extraction from the mantle than does the consideration of the (homogenised and generally fractionated) compositions of extrusives alone.

Melt generation and aggregation at spreading centres

Melting at oceanic spreading centres is widely thought to be a polybaric, near-fractional, process and thus a wide variety of melt compositions must be generated within the melting column (e.g. Klein and Langmuir 1987; Johnson et al. 1990). However, the variation in melt compositions erupted is generally quite small. This

requires that somewhere within the magma plumbing system the diverse melts are mixed together, or aggregated, to produce a much less variable 'end-product'. Much geochemical information is 'lost' because of this mixing. Clearly, even the extrusives are not 'completely aggregated' because lavas with different parental compositions erupt in close spatial and temporal proximity. Understanding where aggregation occurs is critical to developing better models of magma plumbing and, in particular, how melts are extracted from the mantle at spreading centres.

One approach to understanding melt generation, extraction and aggregation is through the investigation of the diversity of melt compositions generated and how these vary spatially within the magma plumbing system. For example, melt inclusion studies have demonstrated that there is much more diversity in the melts parental to primitive olivine (e.g. Sobolev and Shimizu 1993) and plagioclase (e.g. Sours-Page et al. 1999) crystals than there is in erupted lavas at normal mid-ocean ridges. The same information can be gained from trace element analysis of cumulus crystal in plutonic rocks formed in the lower crust at spreading centres (e.g. Coogan et al. 2000a). This has some advantages over melt inclusion studies in that there is no need to rely on the 'chance' occurrence of melt inclusions and where in the magma plumbing system the crystals formed is somewhat better constrained.

In this study we investigate melt generation and aggregation processes within the Troodos ophiolite principally using the trace element compositions of the cores of cumulus clinopyroxene as indicators of the compositions of melts added to the crust. The Troodos ophiolite was chosen for this study for a number of reasons. Firstly, clinopyroxene was an early crystallising phase in the Troodos ophiolite and, thus, its composition should preserve evidence of the compositional diversity of parental melts added to the crust. This contrasts with normal mid-ocean ridge basalts (NMORB) in which the later crystallisation of clinopyroxene means that it has less chance of recording compositional information about Moho-crossing melt compositions prior to their mixing and fractionation. Also, the presence of clinopyroxene throughout almost all of the Troodos plutonic complex allows it to be used to investigate parental magma compositions in diverse locations. Secondly, previous workers have mapped early and late plutonic suites providing a starting point for sampling. Thirdly, previous studies have concentrated principally on the superbly exposed lava and sheeted dyke sequences that provide a database for the compositional variability of melts extracted from the lower crust. Finally, as a consequence of its strong supra-subduction zone (SSZ) geochemical signature, comparison of the Troodos ophiolite with data from normal mid-ocean ridges may allow insights into the similarities and differences between the magma plumbing system at SSZ spreading centres and normal MORs (i.e. mid-ocean ridges away from the influence of subduction zones).

The Troodos ophiolite

The ~91-Ma (Mukasa and Ludden 1987) Troodos ophiolite has been influential in the development of ideas of mid-ocean ridge processes and ophiolite formation in subduction-related settings. It is a classic SSZ ophiolite as identified principally by its lava geochemistry (e.g. Miyashiro 1973; Pearce et al. 1984; Robinson et al. 1983; Rautenschlein et al. 1985). This is evident both in the major element (e.g. the presence of boninitic lavas, basaltic andesites, andesites and dacites) and trace element (e.g. high large ion lithophile element to high field strength element ratios and low high field strength element abundances for a given degree of differentiation) compositions of the lavas and dykes. There is no evidence that any of the exposed crust has a normal mid-ocean ridge basalt (NMORB) composition. Formation of the ophiolite at a submarine spreading centre is demonstrated by the continuous sheeted dyke complex, abundant pillow lavas and overlying marine sediments. Despite the strong SSZ geochemical signature there is no evidence for an adjacent volcanic arc during the formation of the Troodos ocean crust and the lack of volcaniclastic sediments provides strong evidence that there were no associated subaerial volcanic edifices (e.g. Robertson 1990). A series of drill cores, which recovered almost the entire lava and dyke complexes and ~1.5 km into the plutonic complex (referred to as CY1, CY1A, CY2, CY2A and CY4), have provided an important resource for much of the work in Cyprus. The ophiolite can be broadly divided into two regions, the main ophiolite massif to the north and a structurally and geochemically more complex region to the south. They are divided by the Arakapas Fault Zone, which is believed to have been an transform fault. This study was carried out entirely within the main ophiolite massif north of this fault zone.

A large number of studies have investigated the lava stratigraphy in the Troodos ophiolite. A commonly held view is that there is a lower suite of basaltic–andesite to dacite lavas, referred to as the lower pillow lavas (LPL), which may be aphyric or contain phenocrysts of plagioclase, clinopyroxene, orthopyroxene and/or magnetite. This is overlain by a more primitive basaltic to andesitic upper pillow lava (UPL) suite, which can contain chromite, olivine, orthopyroxene, clinopyroxene and plagioclase phenocrysts (e.g. Cameron 1985; Thy and Xenophontos 1991). However, in reality, there is considerable complexity within the lava stratigraphy with primitive lavas also being common at the base of the lava section in some areas (Taylor 1990; Bednarz and Schmincke 1994; Portnyagin et al. 1997) and interlayered with more typical LPL in other places (Taylor 1990; Sobolev et al. 1993). Some studies have suggested that the changes in lava chemistry with depth in the extrusives record the eruption of an axial and an off-axis suite (e.g. Thy and Moores 1988). In contrast, Baragar et al. (1987) shows that there is no systematic age relationship between dykes with UPL and LPL compositions, indicating that there was no temporal transition between

these magma types. Using this observation, together with palaeomagnetic inclinations (used to infer tectonic rotations), Schouten and Denham (2000) propose that the lava sequence was erupted from a single zone with the upper lavas flowing farther off-axis (up to ~2.5 km) and thus ending up at the top of the lava succession. Thus, vertical stratigraphies through the Troodos lava sequence provide, at best, ambiguous information about temporal changes in magma compositions. It is also noteworthy that in the CY1/1A drill cores the more primitive UPLs have the same Zr/Y ratio as the more differentiated LPLs, suggesting that at least some of the distinction between these suites is simply due to the degree of crystal fractionation. Within, and to the south of, the Arakapas Fault Zone there is a third, boninitic suite of lavas (e.g. McCulloch and Cameron 1983; Rogers et al. 1989). Lavas with these highly depleted compositions have not been described in the main ophiolite massif that we have studied.

The plutonic section of the Troodos ophiolites has also been divided into early and late suites by some workers (Benn 1986; Benn and Laurent 1987; Thy 1987; Dunsworth 1989; Ash 1990). However, based on mineral major element compositions there has been disagreement over whether the divisions within the plutonics correspond with the division of the extrusives (Benn and Laurent 1987; Thy 1987; Dunsworth 1989; Malpas 1990). At a map scale, the plutonic sequence appears to show a general stratigraphic sequence. At the base it is dominated by ultramafic cumulates; these are overlain by mafic cumulates and the most evolved dioritic and trondjemitic lithologies are most abundant near the base of the sheeted dyke complex. The basal 1.5 km of the CY4 drill core shows a similar general stratigraphy, although the depth of the petrological Moho beneath the base of this hole is uncertain (e.g. Thy 1987; Malpas 1990). In detail, however, there is abundant intermixing of the plutonic lithologies; for example, plagiogranites are found adjacent to deep-seated ultramafic cumulates and ultramafic cumulates exist close to the base of the sheeted dyke complex. Decimetre-scale ultramafic and mafic layers also commonly exist adjacent to one another.

Major element compositional variability within the plutonics has been used to investigate magma chamber processes and crustal evolution. These studies have identified compositional layering on a variety of scales within the plutonics. Browning et al. (1989) have documented significant metre-scale cryptic variations in the basal (generally ultramafic) part of the CY4 drill core. Dunsworth (1989) found little cryptic variation on a metre-scale in a 20-m section of layered gabbros northwest of Mt Olympus although a few metre-thick horizons show slight variations in Cr in clinopyroxene. Ash (1990) documents 50–100-m scale variations in whole-rock chemistry in a section of ultramafic cumulates in the Amiandos area. The most detailed, and largest-scale, chemical stratigraphy available is for the CY4 drill core in which Thy (1987) documents various cryptic variations on a 100-m scale. These variations are more strongly developed in the uppermost part of the core within gabbronorites, but are present throughout the core.

In this study the plutonic complex was re-examined and sampled in the field and, to a much lesser extent, in the CY4 drill core (Fig. 1, Tables 1, 2, 3, 4 and 5). Samples were collected from nearly the entire outcrop area of the main Troodos plutonic complex (north of the Arakapas Fault Zone) to provide an overview of the trace element variability within the lower crust. Samples were collected from all previously mapped units using the maps of Wilson (1959), Benn (1986), Benn and Laurent (1987), Dunsworth (1989), Ash (1990) and Malpas and Brace (1987). Sampling was restricted to the main ophiolite massif, north of the Arakapas Fault Zone, both because this is the area in which previous mapping identified early and late plutonic suites and also to avoid the complexities associated with the area within and to the south of the Arakapas Fault Zone.

Analytical techniques

The major element compositions of the cores of clinopyroxene, plagioclase and olivine crystals were determined using a JEOL 8600 electron microprobe at the University of Leicester. A 30-nA beam current, 15-kV accelerating voltage and 10-μm spot size were used for all analyses. A ZAF correction procedure was used to reduce the raw data.

The trace element compositions of the cores of cumulus clinopyroxene crystals were determined using a Cameca 4f ion microprobe at the University of Edinburgh. Crystals were chosen for analysis on the basis of being the largest (unaltered) clinopyroxene in a thin section and, thus, the most likely to be a cut through the centre of a crystal. Even if ~50% of the volume of a crystal is zoned this only constitutes the outer ~20% of the diameter of the crystal, making it likely that the cores of crystals can be identified in this way. Calibration was performed against NIST 610 using element abundances from Pearce et al. (1997). A ~15-nA beam current produced a spot size of ~30 μm. A 75-eV offset energy was used to reduce molecular interferences and the remaining interferences, such as light rare earth element (LREE) oxides on heavy (H)REEs, were corrected offline. Counting times were varied between samples with the aim of maintaining a precision of better than 15% relative on the lowest abundance elements (LREE), leading to total counting times of up to 250 s on these elements in some samples. All data are reported in Tables 1, 2, 3, 4 and 5.

Whole-rock trace element compositions of dykes cutting the plutonics were determined by ICP-MS using a Perkin Elmer Elan 5000 at Cardiff University. Samples were dissolved using a standard $HF–HNO_3$ dissolution procedure. Calibration was performed using commercial elemental solutions and international rock standards were run as an external check of the data quality.

Field observations

Figure 1 shows the distribution of plutonic lithologies in the area north of the Arakapas Fault Zone and the locations of the samples used in this study. The Pleistocene and Recent uplift of Mt Olympus (e.g. Robertson 1990), which led to the exposure of the deeper plutonic and residual mantle parts of the ophiolite, was accommo-

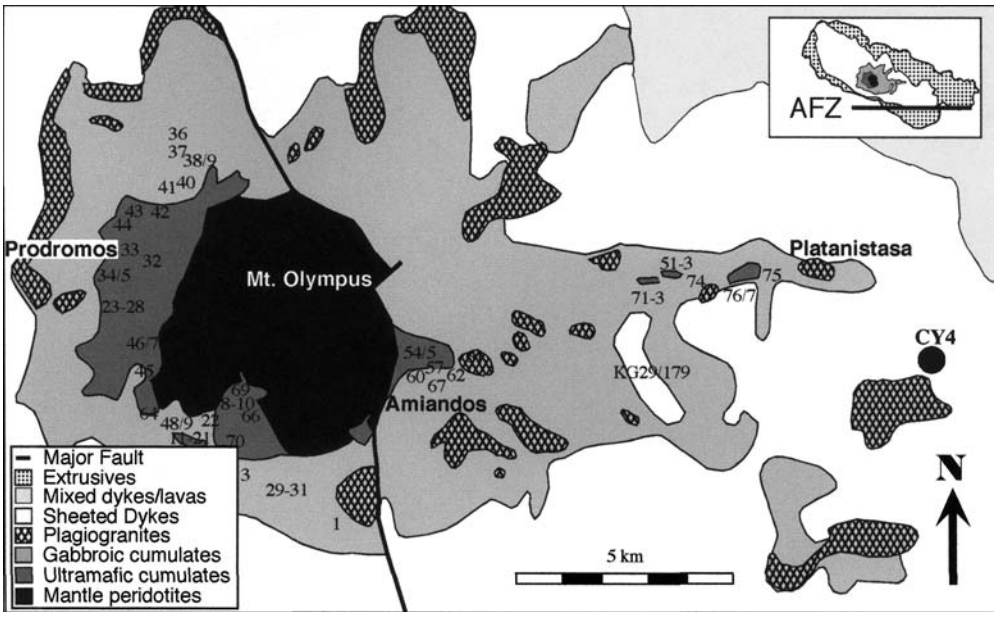

Fig. 1 Simplified map showing the distribution of plutonics in the main part of the Troodos ophiolite (north of the Arakapas Fault Zone) and the location of the samples used in this study (modified from the Geological Survey of Cyprus Map 1995). Sample numbers prefixes 99CL are excluded for clarity. Note that the samples come from almost the entire extent of the exposed plutonic section of the main ophiolite massif. The *inset* shows the Troodos ophiolite with the plutonic section at the centre of a dome-like structure with dykes and then lavas distributed concentrically around it. Also shown is the location of the Arakapas Fault Zone (*AFZ*)

dated by significant faulting along the eastern side of Mt Olympus (Fig. 1). This means that it is difficult to establish a plutonic pseudo-stratigraphy except within the CY4 drill core and it also makes accurate calculation of the thickness of the Troodos crust difficult. Three estimates of crustal thickness can be made. Firstly, Vine and Smith (1990) show that geological reconstruction of CY1, CY1a and CY4 produces a stacked crustal section 3.56 km thick "with little more than 100 m of the section missing". This reconstruction produces a systematic variation in rock physical properties (magnetics, density, elasticity and conductivity) with depth supporting the 'stacked' nature of these drill cores. Vine and Smith (1990) suggest that the base of CY4 is probably near the base of the crust indicating a ~4-km-thick crustal section. Secondly, regional mapping led Wilson (1959) to draw cross sections with ≤ 2 km of plutonics and ≤ 2.5 km of dykes and lavas, suggesting a total crustal thickness of ≤ 4.5 km. A maximum thickness (apparent rather than true thickness) of the plutonics is defined by their horizontal outcrop extent to the west of Mt Olympus. In this region, the foliation within the plutonic section varies smoothly from east to west, implying that the uplift of Mt Olympus was principally taken up by doming rather than faulting (Dunsworth 1989). The width of the outcrop of plutonics here is ~5 km placing an upper limit on the thickness of the plutonic suite and thus a maximum crustal thickness is 7.5 km. Finally, south of the Arakapas Fault Zone the crustal thickness has been estimated at ~4 km (MacLeod 1990). In summary, we suggest that the total crustal thickness is probably < 5 km and is certainly ≤ 7.5 km.

The previous studies that have divided the plutonics into early and late suites (Benn 1986; Benn and Laurent 1987; Dunsworth 1989; Ash 1990) have used three principal field criteria to define mappable plutons: (1) patches of one lithology or grain size in a body of another lithology or grain size, which are interpreted as xenoliths; (2) the coexistence of plutonics in which the layering is folded and contorted and those in which it is not interpreted as indicative of deformation after formation of the folded plutonics and before formation of the unfolded plutonics; and (3) discordancy of layering and foliation orientations within and between adjacent outcrops. Our re-examination of the Troodos plutonics has revealed no evidence for any significant time interval between the bodies mapped as early and late suites. Firstly, features interpreted as xenoliths of other intrusions (e.g. Fig. 5 of Malpas et al. 1989) have major and trace element compositions identical to their hosts. This suggests that either complete equilibration was achieved, or fortuitous similarities existed between their parental melt compositions, or they are not xenoliths (e.g. samples 99CL74a and b; Tables 1, 2, 3, 4 and 5). Although these alternatives cannot be unambiguously distinguished, the compositional similarities between so-called xenoliths and host raises sufficient doubt about the origin of the 'xenoliths' that they cannot be considered as strong evidence for multiple magma chambers. Furthermore, the existence of xenoliths does not require a significant time interval between the formation of the 'xenoliths' and 'host'. Secondly, we find no field or microstructural evidence for significant crystal plastic deformation in any of the plutonic rocks (as exists in oceanic gabbros from slow-spreading ridges; e.g. Cannat 1991). Instead, there is copious evidence of magmatic deformation (e.g. folding and shearing of layering, strong mineral foliations and lineations), which is defined by the orientation of unstrained elongate magmatic crystals. Magmatic deformation may be heterogeneous within a magma chamber (e.g. slumping at the wall, but not at the floor) and, thus, cannot be used as evidence

Table 1 Compositions of all clinopyroxene crystals analysed in this study along with sample modes (visually estimated from thin sections)

Sample prefix	99CL													
Sample	1		8		9		10		11		12		13	
crystal mode (%)	a	b	a	b	a	b	a	b	q	b	a	b	a	a
ol			20	20			10	10	55	55			90	90
opx	35	35	80	80	40	40	50	50	45	45	25	25	10	10
opx	5	5									15	15		
plag	60	60			60	60	40	40			60	60		
wt%														
SiO_2	52.3	53.7	53.7	53.3	53.7	53.3	53.7	54.0	53.9	53.4	52.8	53.2	53.8	53.3
TiO_2	0.32	0.14	0.17	0.14	0.21	0.24	0.15	0.18	0.08	0.07	0.16	0.14	0.11	0.14
Al_2O_3	3.2	1.6	2.0	2.5	2.4	2.1	1.9	1.9	2.1	2.4	3.1	1.7	2.0	2.0
Cr_2O_2	0.06	0.20	0.23	0.25	0.22	0.24	0.22	0.15	0.48	0.76	0.06	0.20	0.23	0.25
FeO	7.8	5.1	5.5	5.9	4.7	4.9	4.9	5.1	5.2	4.0	5.2	4.7	4.0	4.3
MnO	0.19	0.14	0.15	0.16	0.21	0.21	0.12	0.12	0.12	0.11	0.15	0.12	0.17	0.12
MgO	16.6	18.6	18.2	18.6	15.7	16.2	17.6	18.1	17.8	18.4	16.7	17.3	17.9	17.5
CaO	19.0	20.7	20.9	18.4	23.5	23.5	21.6	21.7	21.8	21.5	21.9	22.4	22.7	22.3
Na_2O	0.30	0.08	0.13	0.17	0.14	0.15	0.13	0.12	0.14	0.06	0.20	0.08	0.08	0.28
Total	99.8	100.3	101.1	99.3	101.9	100.9	100.4	101.2	100.6	100.8	100.2	99.8	100.9	100.3
ppm														
Sc	71	101	82	85	87	88	78	79	77	70	91	82	90	79
Ti	723	1,865	753	795	804	848	774	767	416	378	665	676	517	427
V	167	294	191	195	206	209	183	179	188	179	218	220	215	193
Cr	1,562	975	1,585	1,842	1,706	1,572	1,222	1,199	3,279	5,413	746	1,241	1,377	1,735
Sr	3.2	4.5	3.3	3.9	3.6	4.0	3.5	3.6	2.2	2.3	3.4	2.6	2.9	3.3
Y	4.6	11.0	5.0	5.1	5.3	5.3	5.2	5.4	2.9	2.3	4.5	4.7	3.5	2.8
Zr	0.93	6.15	1.07	1.10	1.20	1.29	1.26	1.28	0.26	0.28	0.88	0.56	0.30	0.44
La	0.05	0.13	0.03	0.03	0.04	0.04	0.04	0.03	0.01	0.01	0.03	0.01	0.01	0.02
Ce	0.17	0.56	0.15	0.12	0.16	0.17	0.18	0.19	0.04	0.03	0.12	0.08	0.04	0.06
Pr	0.05	0.14	0.05	0.03	0.04	0.06	0.05	0.06	0.01	0.01	0.03	0.03	0.02	0.02
Nd	0.49	1.33	0.38	0.38	0.43	0.46	0.46	0.51	0.11	0.07	0.37	0.27	0.13	0.13
Sm	0.26	0.69	0.28	0.32	0.36	0.35	0.29	0.32	0.12	0.08	0.25	0.22	0.12	0.11
Eu	0.13	0.30	0.12	0.15	0.11	0.15	0.13	0.14	0.07	0.04	0.13	0.11	0.07	0.06
Gd	0.51	1.07	0.55	0.53	0.57	0.65	0.55	0.59	0.30	0.20	0.50	0.46	0.30	0.27
Tb														
Dy	0.80	1.67	0.77	0.84	0.91	0.79	0.88	0.91	0.48	0.41	0.84	0.72	0.57	0.45
Ho	0.18	0.42	0.19	0.22	0.20	0.22	0.21	0.22	0.12	0.09	0.20	0.18	0.13	0.11
Er	0.53	1.25	0.70	0.51	0.51	0.64	0.58	0.65	0.38	0.27	0.48	0.45	0.37	0.29
Tm														
Yb	0.50	1.07	0.49	0.62	0.34	0.52	0.61	0.63	0.39	0.25	0.52	0.61	0.36	0.35
Lu														

for difference in the age of the plutonics (e.g. McBirney and Nicolas 1997). This could also lead to discordance between layering and foliation orientations in different parts of a single magma chamber. Thus, the observation of discordance between layer orientations is, at best, inconclusive evidence for multiple magma chambers. Finally, no chilled margins were identified within the plutonics even where different lithologies exist adjacent to one another. It is thus concluded that field relationships do not provide unequivocal evidence for (or against) the existence of multiple magma chambers that cooled completely prior to the intrusion of later plutons.

Petrography and mineral major element compositions

The plutonic rocks of the Troodos ophiolite range from dunites through to plagiogranites. In this study, the most evolved lithologies have not been considered because the aim was to investigate parental melt compositions; however, the range of lithologies studied is still large (Fig. 2; Tables 1, 2, 3, 4 and 5). Ultramafic samples are dominated by clinopyroxene and/or olivine with lesser amounts of orthopyroxene, plagioclase and Cr-spinel. Mafic samples are generally olivine and Cr-spinel free and orthopyroxene-bearing. No troctolites were observed in the field. The high abundance of ultramafic cumulates and the absence of troctolites indicates a reversal in the order of appearance of clinopyroxene and plagioclase on the low pressure liquidus compared with that in MORB. This suggests either that the parental melt was highly depleted and/or that it had a high H_2O activity, which would have suppressed plagioclase saturation (e.g. Panjasawatwong et al. 1995).

Figure 3 compares the co-variation of clinopyroxene Mg#-Cr_2O_3 and Mg#-TiO_2 in the Troodos plutonics

14		15		16		17		18		19		20		22		
a	b	a	b	a	b	a	b	a	b	a	b	a	b	a	b	b
						65	65							5	5	5
20	20	25	25	30	30	35	35	25	25	25	25	50	50	30	30	30
20	20	15	15	10	10			15	15	15	15			10	10	10
60	60	60	60	60	60			60	60	60	60	50	50	55	55	55
53.1	53.4	63.3	53.6	53.6	53.6	53.5	53.4	54.2	54.3	52.2	52.4	52.2	51.9	53.5	53.5	53.4
0.15	0.22	0.09	0.31	0.19	0.27	0.12	0.23	0.22	0.09	0.44	0.41	0.41	0.46	0.15	0.18	0.14
2.2	2.0	2.5	1.2	1.9	2.0	1.4	2.0	1.7	1.7	1.9	1.5	1.8	2.0	2.1	2.0	2.0
0.09	0.09	0.25	0.22	0.02	0.12	0.51	0.78	0.14	0.14	0.02	0.00	0.00	0.00	0.29	0.29	0.31
6.0	6.3	4.2	5.0	6.3	6.1	3.5	3.1	6.1	5.2	10.8	9.4	9.6	9.9	4.2	4.2	4.2
0.18	0.17	0.11	0.15	0.16	0.18	0.14	0.09	0.15	0.19	0.24	0.27	0.23	0.25	0.10	0.13	0.14
17.0	16.9	17.0	16.4	16.8	16.6	16.9	17.2	17.5	16.4	14.5	14.3	14.3	14.9	18.2	18.0	18.0
21.3	21.3	23.1	23.1	22.2	22.8	23.9	23.8	21.5	23.6	20.4	21.9	21.0	20.4	21.6	21.7	21.8
0.14	0.13	0.12	0.17	0.16	0.21	0.18	0.24	0.25	0.15	0.25	0.25	0.23	0.24	0.14	0.14	0.09
100.1	100.5	100.6	100.1	101.3	101.8	100.0	100.8	101.7	101.8	100.8	100.5	99.8	99.9	100.3	100.1	100.0
91	90	80	97	101	98	77	90	94	88	149	155	135	138	79	83	82
848	973	529	1,321	1,110	1,070	752	935	1,194	840	2,358	2,004	5,183	2,162	687	723	709
230	259	204	289	252	248	172	196	248	211	323	316	410	394	198	198	193
652	867	1,882	1,844	376	686	7,421	5,721	1,551	1,622	162	162	375	302	2,132	2,163	2,092
4.5	3.9	3.0	2.7	4.3	3.2	3.3	3.8	3.5	3.6	4.5	4.1	3.8	4.1	2.6	3.4	2.8
5.3	5.7	3.6	8.8	7.6	6.7	6.1	8.2	9.9	6.3	21.1	23.3	17.1	17.0	4.6	4.7	4.7
1.05	1.66	0.98	2.74	2.80	1.76	1.61	2.14	5.24	2.03	4.63	6.44	6.45	4.45	0.70	0.68	0.69
0.03	0.03	0.02	0.08	0.07	0.05	0.09	0.09	0.14	0.08	0.15	0.16	0.16	0.13	0.02	0.02	0.02
0.16	0.18	0.12	0.33	0.33	0.24	0.26	0.34	0.68	0.36	0.76	0.87	0.77	0.66	0.10	0.11	0.10
0.05	0.05	0.03	0.09	0.08	0.06	0.06	0.09	0.17	0.08	0.20	0.28	0.22	0.18	0.03	0.03	0.03
0.44	0.50	0.23	0.67	0.77	0.73	0.55	0.68	1.16	0.67	1.84	2.50	1.79	1.82	0.24	0.30	0.29
0.31	0.33	0.17	0.54	0.46	0.47	0.39	0.44	0.62	0.38	1.34	1.56	1.13	1.02	0.20	0.27	0.27
0.15	0.15	0.08	0.19	0.22	0.19	0.13	0.21	0.28	0.16	0.50	0.52	0.42	0.38	0.11	0.10	0.13
0.57	0.63	0.35	0.92	0.89	0.83	0.73	0.85	1.10	0.62	2.42	2.68	1.94	1.89	0.49	0.49	0.46
0.95	0.95	0.61	1.52	1.16	1.28	0.93	1.27	1.41	1.03	3.64	4.15	2.88	2.99	0.93	0.86	0.84
0.21	0.21	0.14	0.36	0.31	0.30	0.23	0.30	0.36	0.23	0.78	0.90	0.68	0.67	0.20	0.18	0.16
0.51	0.60	0.36	0.95	0.82	0.73	0.66	0.85	0.94	0.66	2.21	2.53	1.76	1.79	0.50	0.59	0.46
0.62	0.57	0.46	1.02	0.80	0.73	0.68	1.14	1.04	0.85	2.15	2.38	1.80	1.73	0.51	0.53	0.38

with that observed in gabbros from normal mid-ocean ridges. In the relatively primitive samples ($Cr_2O_3 >$ 0.3 wt%) the Troodos clinopyroxenes generally have a higher Mg#, and a lower Ti content, for a given Cr_2O_3 content than clinopyroxene in gabbros from normal mid-ocean ridges. This suggests that, with respect to MORB, the Troodos parental melt was more magnesian and had lower incompatible element abundances, consistent with studies of the lava and dyke geochemistry (e.g. Pearce et al. 1984; Sobolev et al. 1993).

Oxygen fugacity

The sources of supra-subduction zone magmas are generally more oxidised than the MORB source (e.g. Parkinson and Arculus 1999). The partitioning of Fe into plagioclase is strongly dependent on oxygen fugacity because of the higher partitioning of Fe^{3+} into plagioclase (in place of Al^{3+}) than that of Fe^{2+} (e.g. Phinney 1992); thus, the partitioning of iron between plagioclase and coexisting mafic phases can be used as an oxygen barometer. In order to estimate the oxygen fugacity under which crystallisation of the Troodos plutonics took place the oxygen barometer of Sungawara (2001) has been applied to new and published data for coexisting plagioclase and olivine. The results are shown in Fig. 4 in which they are compared with data for gabbros from the Mid-Atlantic Ridge. The values for the Mid-Atlantic Ridge gabbros are similar to, or slightly higher than, those expected based on direct Fe^{3+}/Fe^{2+} measurements for primitive MORB glasses (Christie et al. 1986). The higher values may either indicate a slight offset of the barometer calibration to higher fO_2 values, or that the magma that crystallised the Mid-Atlantic Ridge gabbros was

Table 2 Compositions of all clinopyroxene crystals analysed in this study along with sample modes (visually estimated from thin sections)

99CL														
Sample	23		24		27A	27B	28		30		31		34	
mode	a	a	a	a	a	b	a	b	a	b	a	b	a	b
ol			50	50	5				60	60			30	30
cpx	40	40	30	30	90	100	80	80	30	30	30	30	55	55
opx			20	20			20	20			10	10	15	15
plag	60	60			5				10	10	60	60		
wt%														
SiO_2	53.5	53.2	54.7	55.1	54.8	54.0	54.1	54.9	53.8	53.8	54.2	54.2	54.9	55.4
TiO_2	0.09	0.11	0.03	0.00	0.04	0.07	0.02	0.06	0.12	0.11	0.13	0.13	0.05	0.04
Al_2O_3	1.1	1.4	0.8	0.8	1.1	1.6	1.0	1.2	2.4	2.2	0.8	0.8	1.1	0.7
Cr_2O_3	0.07	0.07	0.70	0.74	0.50	0.51	0.56	0.55	0.89	0.94	0.07	0.07	0.50	0.38
FeO	6.6	6.3	3.1	3.0	3.7	3.8	3.4	3.5	3.7	3.4	4.9	4.9	3.6	4.0
MnO	0.22	0.26	0.09	0.09	0.13	0.13	0.14	0.13	0.11	0.12	0.17	0.17	0.09	0.15
MgO	16.1	15.9	19.5	19.5	19.9	18.0	19.0	18.8	18.9	18.4	16.7	16.7	19.0	21.2
CaO	22.7	22.8	22.1	22.0	20.8	22.4	22.1	22.4	21.3	22.0	23.6	23.6	22.3	19.3
Na_2O	0.07	0.07	0.09	0.07	0.05	0.07	0.08	0.07	0.09	0.09	0.06	0.06	0.07	0.03
Total	100.5	100.2	101.0	101.3	101.1	100.5	100.5	101.6	101.2	101.1	100.7	100.7	101.5	101.2
ppm														
Sc	96	100	30	31	41	48	41	41	63	58	101	98	48	38
Ti	546	528	171	183	230	335	219	241	444	410	1.174	1.003	238	162
V	290	291	75	80	106	136	100	100	153	141	295	262	121	85
Cr	515	574	4.354	4.724	3.150	3.202	3.470	3.625	5.969	5.811	612	616	3.001	2.362
Sr	1.9	1.9	1.2	1.5	1.2	1.4	1.3	1.2	2.1	2.1	3.9	3.9	1.2	1.0
Y	3.9	4.0	0.8	0.9	1.3	2.2	1.4	1.5	2.7	2.4	7.2	6.3	1.4	0.8
Zr	0.35	0.34	0.13	0.15	0.14	0.31	0.16	0.16	0.50	0.43	1.44	1.15	0.13	0.07
La	0.02	0.01	0.01	0.01	0.01	0.01	0.01	0.01	0.01	0.01	0.06	0.05	0.01	0.00
Ce	0.06	0.06	0.02	0.02	0.03	0.05	0.03	0.03	0.05	0.05	0.27	0.20	0.03	0.01
Pr	0.01	0.01	0.01	0.01	0.01	0.01	0.01	0.01	0.02	0.01	0.06	0.05	0.01	0.00
Nd	0.16	0.14	0.02	0.03	0.07	0.12	0.05	0.07	0.15	0.14	0.65	0.50	0.08	0.03
Sm	0.14	0.17	0.03	0.02	0.06	0.10	0.05	0.05	0.15	0.13	0.43	0.38	0.05	0.03
Eu	0.10	0.06	0.02	0.01	0.02	0.03	0.02	0.03	0.07	0.06	0.17	0.17	0.03	0.01
Gd	0.36	0.33	0.07	0.10	0.11	0.19	0.13	0.16	0.24	0.19	0.79	0.74	0.11	0.06
Tb														
Dy	0.63	0.69	0.15	0.15	0.17	0.42	0.24	0.26	0.42	0.42	1.07	1.06	0.22	0.13
Ho	0.14	0.17	0.03	0.04	0.06	0.08	0.06	0.06	0.09	0.10	0.27	0.25	0.04	0.03
Er	0.42	0.52	0.11	0.10	0.14	0.26	0.17	0.16	0.31	0.26	0.76	0.86	0.14	0.10
Tm														
Yb	0.42	0.52	0.14	0.18	0.17	0.30	0.17	0.19	0.35	0.24	0.83	0.75	0.16	0.10
Lu														

slightly more oxidised than primitive MORB. Either way, the systematic difference between the Mid-Atlantic Ridge and Troodos plutonics, with the Troodos plutonics recording oxygen fugacities slightly more than one log unit higher, is consistent with the inference of a SSZ setting based on basalt geochemistry. The larger range in fO_2 recorded by the Troodos plutonics may suggest more variation in parental melt composition than at normal MORs.

Clinopyroxene trace element characteristics

Clinopyroxene crystal cores contain a wide range of trace element abundance (e.g. from 20 ppb to 5 ppm Nd). If we are to use this variation to investigate the generation and aggregation of their parental melts then the clinopyroxene compositions must record equilibrium with their parental melt and the partitioning between melt and crystals must have been approximately constant. Equilibrium with the parental melt requires that the crystals were in equilibrium with the melt when they grew and that later volume diffusion did not modify their compositions, for example, by re-equilibration with trapped melt.

Several lines of evidence suggest that the first requirement is likely. Firstly, experimental studies have shown that surface equilibrium between melt and clinopyroxene is highly probable during crystal growth (Watson 1996). Even using the slowest available REE diffusion data in clinopyroxene at temperatures $>1{,}210$ °C disequilibrium growth is unlikely at natural growth rates (Van Orman et al. 2001). Secondly, disequilibrium partitioning leads to an enrichment of high charge-to-mass elements over lower charge-to-mass elements (Shimizu 1981). Thus, if variable degrees of disequilibrium lead to variations in the effective partition coefficients during the crystallisation of different samples

35		36		37		39		40				41		43		45
a	b	a	b	a	b	a	b	a	a	a	a	a	b	a	b	a
								70	70	70	70			30	30	
25	25	25	25	20	20	25	25	30	30	30	30	25	25	70	70	70
15	15	15	15	15	15	20	20					15	15			
60	60	60	60	65	65	55	55					60	60			
53.5	53.8	54.1	54.5	52.7	53.2	52.8	53.0	54.3	54.1	53.5	51.9	53.3	53.0	54.7	54.2	53.1
0.25	0.25	0.24	0.21	0.32	0.22	0.30	0.43	0.02	0.09	0.03	0.03	0.14	0.18	0.03	0.04	0.12
1.7	1.5	1.8	1.8	2.0	1.9	1.9	1.8	1.6	1.5	1.6	1.3	1.9	1.7	1.2	1.3	2.2
0.07	0.02	0.05	0.03	0.09	0.17	0.08	0.06	0.98	0.94	0.95	0.82	0.15	0.16	0.86	0.81	0.39
8.7	8.7	6.0	5.6	7.6	8.5	8.0	7.9	2.9	2.7	2.5	3.0	7.1	6.9	3.7	3.2	3.9
0.21	0.21	0.19	0.20	0.21	0.21	0.20	0.15	0.11	0.11	0.10	0.12	0.22	0.17	0.08	0.11	0.11
14.9	14.9	17.3	16.8	15.7	16.1	15.4	15.8	19.0	18.6	18.0	21.0	16.5	16.5	20.4	18.6	18.2
22.3	22.5	22.4	22.9	21.9	21.0	22.3	21.6	22.1	22.6	23.4	20.1	20.9	21.5	20.2	22.7	22.0
0.29	0.26	0.20	0.20	0.20	0.19	0.27	0.23	0.09	0.09	0.12	0.10	0.19	0.19	0.08	0.07	0.12
102.1	102.2	102.2	102.2	100.7	101.4	101.2	100.9	101.1	100.6	100.3	98.3	100.4	100.3	101.2	101.0	
129	174	106	108	93	148	114	115	41	39	42	39	92	89	37	42	75
1.795	6.874	1.108	1.155	1.095	1.175	1.851	1.489	257	258	275	236	777	833	207	303	
397	777	255	275	221	271	348	332	91	92	96	90	228	210	87	112	165
240	389	348	271	1.363	867	600	558	5.813	5.790	6.142	5.884	969	870	4.979	5.153	2.604
4.0	13.7	3.3	3.8	4.0	3.8	3.5	3.8	2.9	2.9	3.4	2.6	3.1	2.9	0.7	0.8	3.8
13.5	39.2	7.4	7.8	7.3	9.4	13.1	10.4	1.4	1.4	1.5	1.3	6.2	6.3	1.2	1.6	3.8
5.89	18.44	2.02	2.39	2.07	2.45	5.25	3.60	0.33	0.32	0.36	0.26	1.33	1.99	0.11	0.18	1.05
0.23	0.75	0.04	0.06	0.10	0.16	0.14	0.11	0.01	0.01	0.01	0.01	0.07	0.08	0.00	0.00	0.03
0.95	3.20	0.21	0.28	0.39	0.66	0.72	0.57	0.04	0.05	0.06	0.05	0.28	0.41	0.01	0.01	0.14
0.21	0.70	0.07	0.08	0.08	0.15	0.19	0.15	0.01	0.01	0.01	0.01	0.07	0.11	0.00	0.00	0.04
1.64	5.24	0.69	0.73	0.72	0.98	1.58	1.32	0.13	0.08	0.12	0.14	0.48	0.68	0.03	0.04	0.33
0.89	2.58	0.45	0.46	0.46	0.65	0.94	0.68	0.11	0.09	0.06	0.06	0.32	0.37	0.04	0.05	0.24
0.34	0.89	0.19	0.21	0.21	0.26	0.28	0.24	0.04	0.04	0.03	0.04	0.13	0.15	0.02	0.03	0.13
1.55	3.99	0.72	0.88	0.80	1.04	1.38	1.13	0.12	0.18	0.16	0.13	0.67	0.72	0.09	0.16	0.45
2.32	6.21	1.27	1.36	1.19	1.58	2.27	1.70	0.18	0.22	0.29	0.26	0.89	1.00	0.24	0.29	0.68
0.54	1.37	0.31	0.32	0.28	0.34	0.49	0.37	0.04	0.05	0.06	0.06	0.23	0.24	0.04	0.06	0.14
1.30	3.79	0.88	0.89	0.67	1.03	1.28	1.07	0.15	0.16	0.16	0.12	0.63	0.86	0.17	0.21	0.37
1.53	3.93	0.81	0.88	0.85	0.99	1.54	1.09	0.18	0.21	0.13	0.21	0.75	0.67	0.21	0.24	0.39

then elements such as Zr and Nd would be fractionated. Instead, the data show an excellent one-to-one correlation between these elements. Thirdly, disequilibrium partitioning leads to an increase in the effective partition coefficient over the equilibrium partitioning for incompatible elements with all partition coefficients tending to unity. In contrast, a key characteristic of the Troodos clinopyroxenes is their very low incompatible element concentrations and the low ratios of more-to-less incompatible elements. Fourthly, comparison of the compositions of the clinopyroxene crystals in the Troodos plutonic suite with those of cumulate clinopyroxene from the present-day oceans should allow direct comparison of the parental melt compositions (e.g. Fig. 3). This is true unless crystallisation rates were substantially different during formation of the Troodos ophiolite than they are at either the slow- or the fast-spreading Mid-Atlantic Ridge and East Pacific Rise. Finally, for disequilibrium growth to lead to the wide range of trace element crystallisation of these plutonic rocks would have had to occur at very different rates, which does not seem likely based on the similar, and coarse, grain sizes and the lack of chilled margins in the field.

Significant diffusive elemental transport within the volume of the clinopyroxene crystals post-crystallisation is unlikely to have been important in modifying the trace element compositions of clinopyroxene crystal cores as all of the trace elements analysed in this study have very slow diffusion rates (Sneeringer et al. 1984; Van Orman et al. 2001). In support of this, Coogan et al. (2000b) demonstrate that sub-solidus diffusion cannot have modified zoning profiles in clinopyroxene in plutonics from the Mid-Atlantic Ridge.

Large variations in distribution coefficients between crystals seem unlikely. This is because the variations in clinopyroxene major element compositions – the dominant control on the distribution coefficients (Wood and Blundy 1997) – are relatively small. For example, the

Table 3 Compositions of all clinopyroxene crystals analysed in this study along with sample modes (visually estimated from thin sections)

99CL															
Sample mode	45	47		48			49		52	53		63	54A	54B	
	b	a	b	a	b	c	a	b	a	a	b	b	a	b	c
o1	30			50	50	50			30				85	70	70
cpx	70	20	20	25	25	25	25	25	20	50	50	50	15	15	15
opx		20	20	25	25	25	15	15	20	50	50	50		15	15
plag		60	60				60	60	30						
wt%															
SiO_2	53.4	53.5	53.8	53.9	54.2	54.1	53.1	52.3	53.0	51.4	51.9	52.4	52.5	53.9	53.8
TiO_2	0.17	0.17	0.21	0.37	0.20	0.16	0.10	0.42	0.40	0.67	0.61	0.42	0.03	0.04	0.04
Al_2O_3	2.3	1.8	1.9	2.2	1.9	2.4	0.8	1.6	2.7	2.4	2.3	2.2	2.3	2.6	2.5
Cr_2O_3	0.39	0.05	0.12	0.96	0.69	0.83	0.00	0.02	0.21	0.16	0.24	0.23	1.01	1.00	0.97
FeO	4.2	6.3	7.0	3.3	3.1	3.3	9.3	9.9	7.2	8.4	7.6	6.8	3.4	3.8	3.4
MnO	0.12	0.18	0.16	0.09	0.12	0.10	0.21	0.26	0.16	0.29	0.23	0.19	0.07	0.13	0.12
MgO	18.1	16.9	17.4	17.8	18.1	17.5	14.4	14.0	17.2	15.2	16.1	16.8	19.0	20.3	18.7
CaO	22.0	21.9	21.5	23.0	23.3	23.5	22.4	21.8	20.5	20.7	20.5	20.6	21.6	19.5	21.9
Na_2O	0.08	0.18	0.17	0.33	0.31	0.15	0.20	0.25	0.21	0.25	0.19	0.18	0.11	0.09	0.10
Total	100.7	101.0	102.1	101.9	101.9	102.0	100.6	100.6	101.5	99.5	99.6	99.8	100.0	101.4	101.5
ppm															
Sc	84	90	91				166	135	118				60	57	57
Ti	727	1.030	974	1.043	386	1.806	800	2.011	1.976	3.903	2.771	1.958	263	260	271
V	183	222	220	180	102	193	234	279	303	349	299	246	155	152	154
Cr	2.220	698	700	5.592	3.882	4.530	164	119	1.316	806	1.580	1.524	6.748	6.375	6.255
Sr	3.4	4.0	3.9	3.8	5.7	4.7	4.3	6.3	4.6	5.8	5.3	5.0	2.3	1.9	1.8
Y	4.1	7.0	6.2	8.5	4.6	14.9	27.8	19.2	12.3	22.7	15.4	11.1	1.7	1.8	1.6
Zr	0.97	1.90	1.53	3.96	7.01	11.53	12.40	8.69	4.75	10.47	6.07	4.29	0.24	0.30	0.30
La	0.02	0.06	0.06	0.14	0.24	0.31	0.35	0.28	0.09	0.21	0.14	0.11	0.01	0.01	0.01
Ce	0.12	0.32	0.26	0.58	0.59	1.37	1.71	1.03	0.52	1.21	0.76	0.53	0.03	0.03	0.02
Pr	0.02	0.07	0.07	0.13	0.13	0.32	0.40	0.25	0.14	0.31	0.19	0.18	0.01	0.01	0.01
Nd	0.31	0.73	0.60	1.10	0.63	2.29	3.42	2.17	1.37	2.99	1.71	1.30	0.06	0.06	0.04
Sm	0.27	0.41	0.40	0.62	0.39	1.23	2.07	1.26	0.83	1.59	1.08	0.85	0.08	0.08	0.06
Eu	0.13	0.17	0.17	0.22	0.14	0.42	0.45	0.40	0.38	0.57	0.43	0.32	0.03	0.03	0.03
Gd	0.52	0.79	0.68	0.97	0.41	1.99	3.39	2.16	1.44	3.13	1.80	1.52	0.14	0.15	0.13
Tb				0.20	0.12	0.38				0.55	0.42	0.29			
Dy	0.75	1.14	0.98	1.31	0.75	2.70	5.02	3.40	2.16	4.38	2.60	1.86	0.28	0.31	0.29
Ho	0.18	0.26	0.22	0.29	0.18	0.59	1.06	0.77	0.50	0.88	0.56	0.43	0.07	0.07	0.07
Er	0.44	0.70	0.70	1.01	0.55	1.70	3.00	1.81	1.42	2.38	1.63	1.18	0.18	0.18	0.17
Tm				0.15	0.07	0.23				0.35	0.24	0.15			
Yb	0.51	0.75	0.56	0.86	0.58	1.84	2.79	2.24	1.39	2.58	1.98	1.06	0.24	0.24	0.14
Lu				0.09	0.07	0.21				0.29	0.22	0.15			

model of Wood and Blundy (1997) to the clinopyroxene major element compositions predicts $< 3\%$ variation in the distribution coefficient for Nd. Furthermore, there is no correlation between clinopyroxene Ca content and the abundance of incompatible elements despite Ca being critical to the partition coefficient (Gaetani and Grove 1995; Wood and Blundy 1997).

Spatial distribution of clinopyroxene trace element compositions

There is no consistent variation in clinopyroxene compositions between plutonics previously mapped as the early and late suites either within a single map area or across the ophiolite as a whole. The most depleted clinopyroxene trace element signatures are observed in ultramafic cumulates and these are, in general, more depleted than those of adjacent mafic plutonics even where ultramafic and mafic bodies are intermixed on a 100-m scale. However, not all primitive ultramafic cumulates contain depleted clinopyroxene and some rare primitive gabbroic samples also contain clinopyroxene with very depleted trace element compositions. No spatial ordering of clinopyroxene trace element systematics is evident on a map scale, although mappable ultramafic bodies enclosed within high-level gabbronorites (samples 99CL72 and 99CL76; Fig. 1) contain clinopyroxene crystals that are not as depleted as the clinopyroxene in most of the other ultramafic samples studied. Instead the clinopyroxene in these high-level ultramafics have compositions similar to that of clinopyroxene in the surrounding gabbronorites. Despite their high structural level, the parental melt for these bodies was primitive as shown by the high Cr content and $Mg^{\#}$ of clinopyroxene. In summary, ultramafic lithologies are more common at deeper structural levels and those found at deeper structural levels generally, but not invariably, contain more depleted clinopyroxene.

55				57		60		61		62			64		66		
a	a	b	b	a	b	a	b	a	b	a	a	b	a	b	a	a	b
85	85	60	60					5	5	20	20	20			25	25	25
15	15	25	25	100	100	40	40	30	30	60	60	60	25	25	70	70	70
		15	15			25	25	15	15	10	10	10	15	15			
						35	35	50	50	10	10	10	60	60	5	5	5
53.8	54.2	53.3	53.4	53.9	54.0	53.1	52.8	53.2	52.6	53.1	53.1	52.9	53.2	53.3	53.6	53.5	54.0
0.00	0.03	0.05	0.04	0.01	0.08	0.07	0.16	0.11	0.14	0.09	0.11	0.32	0.13	0.07	0.06	0.27	0.03
1.9	2.1	1.9	1.9	1.8	2.4	2.0	2.0	2.1	2.0	2.5	2.4	2.6	0.8	0.5	2.0	2.5	1.8
0.65	0.94	0.95	0.94	0.93	0.96	0.66	0.33	0.46	0.52	0.92	0.63	0.36	0.04	0.06	0.70	0.18	0.66
3.6	3.7	3.5	3.4	2.7	2.8	4.9	5.2	4.8	5.0	4.6	4.0	5.4	9.2	7.6	4.9	5.4	4.1
0.13	0.12	0.14	0.11	0.06	0.15	0.15	0.15	0.16	0.12	0.16	0.11	0.11	0.26	0.25	0.16	0.14	0.14
19.6	19.7	19.6	18.7	17.3	17.2	17.2	17.0	17.1	17.1	17.4	16.9	16.5	14.0	14.8	17.2	16.4	19.3
20.7	20.3	20.5	21.5	24.1	23.7	22.5	22.5	21.9	22.0	22.3	23.9	22.7	22.8	22.9	22.6	22.9	21.1
0.09	0.06	0.08	0.09	0.09	0.14	0.20	0.22	0.16	0.20	0.23	0.19	0.23	0.18	0.18	0.18	0.20	0.08
100.7	101.1	100.0	100.1	100.9	101.6	100.7	100.4	100.1	99.9	101.3	101.4	101.2	100.6	99.8	101.2	101.4	101.3
47	48	61	62	46	50												62
206	222	280	287	200	347	317	922	891	734	723	630	492	1.023	1.053	122	131	403
117	128	160	162	111	129	105	242	189	142	182	180	105	265	239	57	63	164
5.395	5.769	6.539	6.570	5.870	5.817	4.449	1.467	1.864	3.752	4.449	4.198	1.467	190	806	4.117	4.149	3.583
1.6	1.9	1.7	1.8	2.6	2.9	2.5	3.7	4.2	4.0	3.1	2.9		6.6	5.5	1.2	1.6	1.9
1.2	1.2	1.9	1.8	1.3	2.3	2.5	5.3	5.5	4.7	4.7	4.1	1.5	31.4	8.0	0.6	0.8	2.6
0.21	0.19	0.30	0.31	0.26	0.57	0.59	1.49	1.72	1.41	0.94	0.73	0.39	16.28	3.90	0.13	0.15	0.43
0.01	0.01	0.01	0.01	0.01	0.03	0.04	0.07	0.06	0.09	0.03	0.03	0.01	0.75	0.16	0.01	0.02	0.01
0.02	0.02	0.03	0.02	0.04	0.09	0.17	0.23	0.31	0.29	0.16	0.12	0.02	3.14	0.58	0.02	0.03	0.04
0.00	0.01	0.01	0.01	0.01	0.02	0.04	0.06	0.09	0.08	0.03	0.04	0.00	0.68	0.13	0.01	0.01	0.01
0.03	0.04	0.08	0.05	0.07	0.16	0.31	0.44	0.59	0.54	0.45	0.34	0.03	4.91	0.97	0.04	0.07	0.12
0.04	0.05	0.06	0.07	0.04	0.08	0.17	0.37	0.38	0.29	0.28	0.23	0.02	2.30	0.51	0.09	0.09	0.11
0.02	0.03	0.04	0.04	0.03	0.06	0.07	0.15	0.16	0.15	0.13	0.13	0.01	0.42	0.22	0.01	0.03	0.05
0.09	0.13	0.18	0.18	0.14	0.23	0.29	0.65	0.81	0.63	0.53	0.50	0.08	3.82	0.99	0.03	0.11	0.22
						0.07	0.13	0.15	0.12	0.09	0.10	0.02	0.73	0.24	0.02	0.02	
0.16	0.24	0.31	0.32	0.24	0.36	0.50	1.01	0.94	0.82	0.73	0.72	0.17	5.54	1.60	0.13	0.14	0.38
0.04	0.05	0.06	0.08	0.04	0.10	0.10	0.24	0.22	0.20	0.22	0.18	0.05	1.20	0.34	0.02	0.03	0.11
0.13	0.14	0.24	0.22	0.19	0.27	0.32	0.63	0.71	0.53	0.50	0.52	0.26	3.51	0.94	0.09	0.11	0.28
						0.05	0.09	0.09	0.08	0.09	0.08	0.05	0.54	0.13	0.02	0.03	
0.13	0.19	0.17	0.18	0.19	0.25	0.45	0.69	0.81	0.54	0.61	0.50	0.41	3.88	1.05	0.09	0.09	0.26
						0.05	0.09	0.09	0.08	0.08	0.09	0.07	0.57	0.13	0.05	0.03	

On a smaller scale, in two places clinopyroxene crystals in adjacent mafic and ultramafic layers within a layered sequence have been analysed (samples 99CL8/9/10 and 99CL52/3; Fig. 1). In both localities layering is on a decimetre-scale. In these instances there is no significant difference in the compositions of the clinopyroxene in the mafic and ultramafic layers. This suggests either a similar parental melt composition with, for example, layering having been formed by physical crystal separation within a magma chamber, or different parent melt compositions with post cumulus dissolution-reprecipitation reactions leading to equilibration between the adjacent layers.

Clinopyroxene trace element systematics

Chondrite-normalised spidergrams of representative clinopyroxene compositions are shown in Fig. 5. The most striking feature of these plots is the greater than two orders of magnitude variation in the abundances of the most incompatible elements. Clinopyroxenes in mafic samples have, on average, slightly higher incompatible element abundances than clinopyroxene in ultramafic samples. All clinopyroxene are characterised by a significant negative Zr anomaly and most by slight negative Ti anomalies. There is a marked positive Sr anomaly in many of the most depleted clinopyroxenes and a negative Sr anomaly in clinopyroxenes with high incompatible element abundances.

Figure 6 shows representative clinopyroxene compositions normalised to the average composition of the most primitive clinopyroxene in gabbros from the MARK area of the Mid-Atlantic Ridge (MAR). Basalts from this region of the MAR are typical NMORB and the clinopyroxene used for normalisation contains ~10,000 ppm Cr suggesting that it is close to being in equilibrium with an unfractionated mantle melt (Coogan et al. 2000a). This normalisation is equivalent to normalising the clinopyroxene parental melts to primi-

Table 4 Compositions of all clinopyroxene crystals analysed in this study along with sample modes (visually estimated from thin sections)

99CL													
Sample	66	67		69			70				72A		72B
mode		c	a	b	a	b	c	a	b	c	c	a	a
ol	25	80	80	30	30	30	70	70	70	70	80	80	40
cpx	70	20	20	65	65	65	30	30	30	30	20	20	60
opx				5	5	5							
plag	5												
wt%													
SiO_2	54.6	52.4	52.7	53.4	53.0	53.0	53.4	53.4	52.8	52.8	52.8	52.8	54.0
TiO_2	0.02	0.07	0.12	0.17	0.13	0.18	0.03	0.01	0.07	0.05	0.16	0.15	0.17
Al_2O_3	1.2	2.0	2.2	2.4	2.8	2.6	3.3	2.9	3.0	2.9	2.5	2.7	2.2
Cr_2O_3	0.57	0.95	0.80	0.42	0.93	0.68	1.23	1.03	1.05	1.10	0.93	0.87	0.71
FeO	3.7	3.3	3.7	3.9	4.3	3.9	3.1	3.3	3.4	3.3	4.1	4.0	4.2
MnO	0.11	0.11	0.11	0.13	0.12	0.15	0.11	0.11	0.11	0.11	0.12	0.09	0.15
MgO	20.3	18.4	18.2	17.5	17.6	17.5	17.4	18.2	18.3	18.4	18.2	18.1	18.3
CaO	20.6	22.3	22.0	22.9	21.7	22.0	23.0	22.4	22.0	22.0	21.3	21.2	21.5
Na_2O	0.10	0.11	0.08	0.16	0.13	0.15	0.11	0.07	0.07	0.08	0.12	0.12	0.12
Total	101.2	99.6	100.0	100.9	100.6	100.1	101.7	101.5	100.8	100.8	100.1	100.0	101.4
ppm													
Sc	34	59	64						64	67	92	89	85
Ti	140	308	417	1,053	804	781	241	228	238	261	1,037	914	867
V	72	144	179	165	138	136	111	110	153	154	221	209	190
Cr	2,968	5,388	5,859	2,836	5,762	4,587	6,451	6,848	7,410	6,828	5,487	5,608	5,705
Sr	1.6	2.1	1.9	6.4	4.6	4.8	2.0	2.1	2.5	2.1	3.6	3.2	3.0
Y	0.9	2.1	2.7	5.6	4.5	4.2	1.5	1.5	1.6	1.7	6.5	5.7	5.4
Zr	0.14	0.35	0.44	3.11	1.54	1.56	0.31	0.35	0.32	0.31	1.49	1.20	1.14
La	0.01	0.01	0.01	0.08	0.06	0.05	0.02	0.01	0.01	0.01	0.04	0.03	0.03
Ce	0.03	0.05	0.05	0.37	0.19	0.22	0.03	0.05	0.03	0.04	0.21	0.16	0.14
Pr	0.01	0.01	0.01	0.09	0.05	0.05	0.01	0.02	0.01	0.01	0.06	0.04	0.04
Nd	0.04	0.10	0.12	0.72	0.68	0.81	0.13	0.06	0.04	0.07	0.53	0.49	0.42
Sm	0.02	0.08	0.11	0.42	0.39	0.31	0.08	0.07	0.06	0.08	0.39	0.27	0.27
Eu	0.01	0.04	0.05	0.16	0.17	0.19	0.04	0.04	0.03	0.04	0.15	0.14	0.13
Gd	0.04	0.20	0.24	0.73	0.63	0.65	0.22	0.14	0.13	0.10	0.72	0.64	0.61
Tb				0.13	0.11	0.15	0.03	0.03					
Dy	0.14	0.38	0.40	1.14	0.77	0.76	0.26	0.21	0.27	0.32	0.99	0.88	0.83
Ho	0.03	0.08	0.12	0.23	0.17	0.16	0.06	0.06	0.07	0.06	0.24	0.21	0.20
Er	0.12	0.25	0.28	0.65	0.50	0.45	0.17	0.21	0.18	0.18	0.77	0.58	0.59
Tm				0.12	0.06	0.07	0.02	0.03					
Yb	0.06	0.28	0.36	0.69	0.57	0.36	0.18	0.27	0.12	0.21	0.72	0.53	0.55
Lu				0.07	0.08	0.06	0.03	0.04					

tive NMORB assuming the same distribution coefficients for both clinopyroxene. This is a reasonable assumption because the major element compositions of the pyroxenes are similar and the crystallisation temperatures are also likely to have been similar. On this basis, Fig. 6 shows that the melts parental to the Troodos plutonic suite (1) were generally more depleted than NMORB, (2) had positive Sr anomalies and (3) were commonly enriched in La and Ce with respect to the middle-REE (e.g. $La_{(n)}/Pr_{(n)} > 1$). This is consistent with the melts being generated from a depleted source into which Sr, and to a lesser extent LREE, were added.

In order to investigate the origins of the variations in incompatible element abundances and ratios Fig. 7 compares the co-variation of clinopyroxene trace element compositions with modelled melting trends and with the compositions of clinopyroxene in gabbros from normal mid-ocean ridges. Details of the modelling methodology are given in the figure caption and Table 6. Although uncertainty in the distribution coefficients (and the approximation of these variables by single values) and starting compositions make all modelling of this kind imperfect, the comparison with the samples from present-day mid-ocean ridges demonstrates that the principal findings are likely to be robust. There is a much wider range of clinopyroxene trace element compositions, extending to much more depleted compositions, than would have crystallised from the lavas for which trace element compositions have been published. This demonstrates that the range of melts parental to the cumulates was far larger than that erupted. The parental melt compositions ranged to more depleted compositions than could be produced by ~30% fractional melting of a homogeneous depleted source if the melts were fully aggregated prior to clinopyroxene crystallisation. This is inconsistent with the relatively thin crust in the Troodos ophiolite (see above) and with the small range of lava compositions. Alternatively, if melts were instanta-

73		74		75			76		77		1239			1345		
b	a	b	a	b	b	a	b	a	b	a	b	c	a	b	a	a
							30	30								
25	25	25	25	30	30	30	65	65	35	35	15	15	15	40	40	40
15	15	15	15	20	20	20	5	5	15	15	25	25	25	15	15	15
60	60	60	60	50	50	50			50	50	60	60	60	45	45	45
54.1	53.8	53.4	53.6	54.1	53.8	54.1	52.9	53.3	53.4	52.8	52.2	52.0	52.9	53.8	53.5	53.7
0.20	0.09	0.34	0.22	0.26	0.26	0.32	0.13	0.09	0.30	0.50	0.48	0.58	0.49	0.18	0.14	0.21
1.9	1.5	1.9	2.0	1.8	2.5	1.9	2.2	2.1	1.7	1.5	1.8	1.8	1.8	2.0	1.9	1.9
0.03	0.14	0.07	0.05	0.16	0.09	0.21	0.33	0.46	0.11	0.06	0.15	0.11	0.18	0.24	0.16	0.05
6.3	4.7	8.3	6.8	5.7	5.7	5.9	4.6	4.7	6.5	8.7	8.2	7.9	8.1	6.0	6.6	7.3
0.12	0.07	0.24	0.19	0.15	0.15	0.19	0.16	0.15	0.15	0.25	0.21	0.21	0.21	0.18	0.19	0.23
17.7	17.6	16.5	16.9	17.6	17.2	17.3	18.2	18.2	17.1	15.4	15.7	15.8	15.6	17.0	17.0	15.6
21.4	22.3	20.7	21.7	21.6	21.4	21.8	21.1	21.3	21.4	21.3	21.0	21.3	21.3	22.1	21.7	22.9
0.09	0.08	0.15	0.14	0.21	0.18	0.21	0.10	0.09	0.12	0.22	0.24	0.21	0.23	0.14	0.12	0.12
101.8	100.3	101.7	101.5	101.7	101.2	102.0	99.9	100.4	100.8	100.7	99.9	100.0	100.8	101.7	101.3	101.9
114	69						78	71	79	126	117	125	128	76	89	74
997	575	2,016	1,559	1,301	1,688	1,837	623	482	964	2,738	2,043	3,111	2,660	621	695	589
300	176	273	324	222	294	245	184	169	200	430	290	355	373	199	229	195
339	1,258	455	465	1,126	819	1,467	2,771	5,543	948	608	1,130	975	1,045	1,384	695	1,880
2.4	2.0	3.9	4.1	3.3	3.9	3.4	2.2	1.8	3.2	3.8	4.1	3.5	3.3	8.1	2.1	2.7
7.4	3.7	10.9	7.7	8.4	10.1	10.5	3.6	2.5	6.0	17.2	17.8	21.0	20.9	3.7	4.2	3.9
0.97	0.64	2.98	1.87	4.04	4.79	14.16	0.61	0.47	1.33	4.62	10.62	8.50	9.50	0.82	0.61	1.20
0.14	0.03	0.08	0.05	0.09	0.10	0.17	0.02	0.01	0.05	0.16	0.26	0.23	0.22	0.05	0.02	0.04
0.23	0.08	0.35	0.25	0.41	0.54	0.75	0.08	0.05	0.22	0.71	1.29	1.25	1.27	0.13	0.10	0.11
0.05	0.02	0.10	0.09	0.10	0.15	0.20	0.03	0.01	0.05	0.21	0.31	0.35	0.37	0.03	0.03	0.05
0.35	0.22	1.45	0.55	0.82	1.11	1.48	0.19	0.16	0.43	1.94	2.59	2.91	2.83	0.28	0.23	0.21
0.32	0.14	0.75	0.49	0.50	0.80	0.72	0.20	0.13	0.31	1.15	1.37	1.43	1.29	0.18	0.18	0.18
0.16	0.07	0.30	0.21	0.21	0.27	0.26	0.09	0.06	0.17	0.32	0.33	0.37	0.39	0.10	0.12	0.07
0.70	0.33	1.20	0.88	1.07	1.30	1.27	0.34	0.32	0.62	1.92	1.87	2.20	2.12	0.43	0.40	0.15
		0.27	0.21	0.21	0.26	0.27										
1.07	0.57	2.12	1.30	1.39	1.92	1.77	0.59	0.54	0.97	2.99	2.77	3.18	3.53	0.72	0.72	0.68
0.29	0.14	0.47	0.32	0.34	0.40	0.43	0.14	0.10	0.23	0.67	0.65	0.78	0.78	0.15	0.15	0.18
0.77	0.43	1.26	0.97	0.94	1.18	1.18	0.37	0.33	0.69	1.88	1.75	2.14	2.50	0.47	0.50	0.38
		0.18	0.12	0.12	0.17	0.18										
0.88	0.40	1.35	0.88	0.76	0.99	1.45	0.43	0.34	0.61	1.69	1.99	2.21	2.22	0.53	0.43	0.50
		0.17	0.12	0.15	0.15	0.16										

neously transported from their source region into the crust, where they precipitated clinopyroxene (probably preceded by an interval of olivine crystallisation) without any mixing with other melt fractions, only 5–10% melting of the depleted source would be required to explain the range of clinopyroxene compositions. Therefore, the data indicate that incompletely aggregated melts were added to the lower crust and crystallised clinopyroxene-bearing cumulates and thus that melt transport within the mantle was inefficient at homogenising the diverse melt compositions generated.

The composition of the mantle source can be investigated using elements that are unlikely to be significantly effected by the addition of a slab-derived component (e.g. Cr, Y, Zr and Ti). Chromium–yttrium systematics (Fig. 7a) show that the melts parental to the Troodos plutonic complex had lower Y abundances, for a given Cr abundance, than clinopyroxene in gabbros from normal mid-ocean ridges. Also, almost all of the primitive (high Cr) Troodos clinopyroxene are more depleted in incompatible elements than in melts produced by 1–15% melting of a fertile source such as the clinopyroxene from the MAR and EPR. Thus, the Troodos parental melts were generated from a source significantly more depleted than the MORB source (see also Fig. 3).

Titanium and zirconium, two immobile incompatible elements, are much more depleted in the Troodos plutonics than in gabbros from normal mid-ocean ridges, ranging to almost an order of magnitude lower Ti abundances and almost two orders of magnitude lower Zr abundances (Fig. 7b). Only a few samples overlap the field of clinopyroxene cores from normal mid-ocean ridges and none of these are from primitive (high Cr) clinopyroxene suggesting that their higher abundances reflect partial crystallisation rather than melting processes. As with the Cr–Y systematics, this requires melting of a more depleted mantle than the MORB source and crystallisation of incompletely aggregated melts.

Table 5 Compositions of all clinopyroxene crystals analysed in this study along with sample modes (visually estimated from thin sections)

CY4													
Sample	1345		1464				1875					1961	
mode	a	a	a	a	b	b	a	b	c	d	c	a	b
ol												20	20
cpx	40	40	45	45	45	45	80	80	80	80	80	65	65
opx	15	15	20	20	20	20	10	10	10	10	10		
plag	45	45	35	35	35	35	10	10	10	10	10	15	15
wt%													
SiO_2	53.5	54.2	54.1	54.8	54.8	54.4	54.2	54.1	55.1	54.5	53.9	55.4	54.2
TiO_2	0.20	0.17	0.06	0.10	0.04	0.07	0.10	0.10	0.06	0.03	0.16	0.04	0.04
Al_2O_3	1.9	2.0	2.0	1.7	2.2	2.1	2.2	2.2	1.4	2.0	2.2	1.4	1.5
Cr_2O_3	0.10	0.19	0.08	0.08	0.27	0.25	0.52	0.54	0.69	0.62	0.53	0.50	0.69
FeO	7.3	6.5	4.8	4.8	4.5	4.2	3.4	3.4	3.0	3.3	4.3	3.4	3.5
MnO	0.17	0.24	0.18	0.14	0.07	0.16	0.12	0.07	0.11	0.08	0.18	0.12	0.05
MgO	16.6	16.5	18.2	18.6	17.5	17.7	17.4	17.6	18.1	17.8	18.7	19.1	18.6
CaO	21.3	22.1	22.3	21.8	23.0	22.8	23.7	23.5	23.3	23.3	21.7	22.3	22.7
Na_2O	0.12	0.12	0.08	0.03	0.04	0.04	0.11	0.08	0.13	0.06	0.13	0.11	0.06
Total	101.2	102.0	102.0	102.4	101.8	101.7	101.6	101.9	101.7	101.8	102.2	101.3	102.3
ppm													
Sc	76	91	76	75	73	71	55	36	40	51	36	49	43
Ti	897	748	365	376	299	417	436	154	162	286	166	210	273
V	245	236	176	180	156	174	132	80	90	113	80	108	100
Cr	2,423	1,669	579	590	1,321	875	3,369	3,677	3,428	2,998	3,695	2,991	4,116
Sr	3.2	2.1	1.7	1.8	1.4	1.6	2.8	1.2	1.3	1.7	1.2	1.9	1.9
Y	5.0	4.8	2.2	2.1	2.1	2.4	2.4	0.9	1.0	1.9	1.1	1.2	1.5
Zr	0.93	0.82	0.29	0.27	0.23	0.69	1.02	0.11	0.15	0.38	0.21	0.17	0.26
La	0.04	0.03	0.01	0.01	0.03	0.03	0.03	0.00	0.02	0.01	0.01	0.01	0.02
Ce	0.13	0.13	0.04	0.05	0.05	0.12	0.13	0.02	0.02	0.06	0.04	0.04	0.05
Pr	0.03	0.04	0.01	0.01	0.02	0.01	0.02	0.00	0.01	0.03	0.01	0.01	0.01
Nd	0.24	0.32	0.11	0.11	0.15	0.14	0.20	0.03	0.03	0.15	0.05	0.07	0.09
Sm	0.22	0.23	0.10	0.10	0.09	0.10	0.14	0.04	0.05	0.14		0.07	0.07
Eu	0.10	0.13	0.05	0.04	0.06	0.05	0.06	0.02		0.02	0.02	0.03	0.04
Gd	0.53	0.59	0.19	0.20	0.21	0.24	0.24	0.07	0.18	0.19	0.15	0.15	0.20
Tb													
Dy	0.75	0.71	0.42	0.43	0.36	0.32	0.40	0.15	0.17	0.28	0.24	0.19	0.30
Ho	0.21	0.15	0.08	0.09	0.07	0.09	0.08	0.03	0.04	0.07	0.05	0.05	0.05
Er	0.74	0.60	0.30	0.28	0.28	0.31	0.22	0.10	0.21	0.27	0.16	0.13	0.15
Tm													
Yb	0.50	0.45	0.28	0.22	0.27	0.31	0.24	0.11	0.19	0.25	0.22	0.08	0.13
Lu													

The redox conditions under which the mantle depletion occurred, prior to the melting event that formed the Troodos crust, can be investigated using the co-variation of V and Ti (Fig. 7c). This is sensitive to the oxidation state of the mantle source because of the decrease in the distribution coefficient for V (D_V) for all mantle minerals with increasing oxygen fugacity (Shervais 1982; Canil 1999; Canil and Fedortchouk 2000). Iron partitioning between plagioclase and olivine suggests that the Troodos gabbros crystallised from a magma with an fO_2 close to 1.5 log units above the quartz–magnetite–fayalite buffer (Fig. 4). Modelling of the co-variation of V and Ti suggests that the initial depletion of the mantle source cannot have occurred under these oxidising conditions as this would have led to lower V abundances in the clinopyroxenes than those observed. Instead, the data can be explained if the initial depletion was under relatively reducing conditions at a normal mid-ocean ridge. This would have produced an increase in the source V/Ti and subsequent remelting of this mantle under more oxidising conditions, followed by crystallisation of clinopyroxene still under these oxidising conditions, would lead to the high V/Ti observed in the clinopyroxene compositions.

Addition of a Sr-rich slab component is suggested by the positive Sr anomalies in some of the more depleted primitive clinopyroxene (Figs. 5 and 6) and the excess Sr with respect to that predicted by modelling the co-variation in Sr and Ce (Fig. 7d). Enriching the source in Sr prior to melting to form the Troodos crust cannot explain the data as melting of the Sr-enriched source produces a depletion trend parallel to that of melting without enrichment (Fig. 7d). Instead, the Sr systematics can be modelled by the progressive addition of Sr during melting, presumably from a slab component. It should be noted that the supra-chondritic Sr/Ce, and the wide range of Sr abundances and Sr/Ce ratios in primitive ($> 3{,}000$ ppm Cr) clinopyroxene cores, indicate that the range of Sr abundances cannot simply be related to plagioclase fractionation.

KG93															
			2073						179			29			
c	d	e	a	b	c	d	e	e	a	b	c	a	b	c	
20	20	20	20	20	20	20	20	20				15	15	15	
65	65	65	80	80	80	80	80	80	30	30	30	30	30	30	
									20	20	20	10	10	10	
15	15	15							50	50	50	45	45	45	
55.3	55.2	53.3	55.2	53.9	53.1	53.5	53.0	53.6	51.9	52.4	51.9	54.6	54.3	53.7	
0.04	0.01	0.09	0.04	0.03	0.06	0.07	0.10	0.04	0.19	0.07	0.06	0.07	0.04	0.14	
1.2	1.5	1.9	0.9	2.0	1.1	1.6	1.7	1.3	2.1	2.2	2.7	0.8	0.9	1.7	
0.50	0.75	0.68	0.15	0.44	0.24	0.50	0.51	0.48	0.69	0.90	0.68	0.06	0.12	0.24	
3.6	2.9	4.3	3.2	3.4	3.4	3.4	3.5	3.2	7.8	5.8	6.8	4.2	4.3	5.1	
0.09	0.12	0.11	0.11	0.11	0.08	0.11	0.11	0.04	0.19	0.15	0.20	0.13	0.14	0.13	
20.0	18.7	18.7	17.5	18.2	17.2	19.1	17.3	18.7	15.6	16.7	16.5	16.9	16.7	16.8	
21.4	23.4	21.2	25.0	23.0	24.3	21.8	24.2	22.6	21.4	21.9	21.1	24.4	24.6	22.9	
0.07	0.09	0.10	0.03	0.10	0.04	0.09	0.37	0.05	0.22	0.20	0.16	0.16	0.06	0.16	
102.6	100.3	102.0	101.2	99.6	100.2	100.8	100.0	100.0	100.3	100.1	101.3	101.1	100.9		
40	36	37	62	48	78	71	83	51	88	66	64	59	60	87	
196	189	177	475	179	507	642	416	288	483	471	333	415	347	728	
85	77	78	134	101	169	181	199	117	220	152	139	87	90	187	
3,582	4,125	3,639	1,724	3,074	2,229	2,942	3,412	2,861	3,671	6,678	3,509	703	652	1,775	
1.4	1.1	1.5	2.1	1.6	2.1	2.4	2.5	1.7	2.6	2.5	2.7	1.2	1.5	2.0	
1.1	1.0	1.0	2.7	1.1	3.9	3.7	4.2	2.3	3.6	3.9	2.7	4.3	2.2	5.0	
0.18	0.18	0.31	0.82	0.15	0.87	1.02	0.64	0.60	0.50	0.78	0.41	1.88	0.66	1.25	
0.00	0.01	0.02	0.03	0.00	0.04	0.02	0.03	0.03	0.10	0.05	0.11	0.07	0.05	0.07	
0.02	0.02	0.08	0.12	0.02	0.16	0.16	0.12	0.09	0.16	0.24	0.26	0.24	0.31	0.16	
0.01	0.01	0.00	0.02	0.01	0.02	0.03	0.04	0.02	0.03	0.03	0.04	0.05	0.01	0.03	
0.03	0.03	0.08	0.26	0.05	0.20	0.30	0.27	0.19	0.07	0.33	0.26	0.45	0.14	0.44	
0.05	0.13	0.07	0.13	0.04	0.19	0.15	0.30	0.19	0.14	0.20	0.14	0.22	0.09	0.25	
0.02	0.01		0.06	0.02	0.11	0.10	0.10	0.06	0.06	0.12	0.07	0.07	0.06	0.10	
0.09	0.09	0.05	0.23	0.10	0.20	0.16	0.36	0.06	0.42	0.41	0.24	0.63	0.42	0.58	
0.17	0.29	0.25	0.47	0.18	0.64	0.77	0.53	0.30	0.75	0.59	0.49	0.67	0.35	0.78	
0.03	0.04	0.02	0.12	0.04	0.12	0.10	0.14	0.09	0.12	0.11	0.10	0.17	0.10	0.24	
0.13	0.13	0.00	0.28	0.13	0.46	0.41	0.32	0.29	0.37	0.41	0.39	0.55	0.20	0.58	
0.11	0.31	0.00	0.34	0.10	0.48	0.41	0.51	0.36	0.42	0.64	0.36	0.50	0.38	0.97	

In summary, the principal observations and first order interpretations of the clinopyroxene trace element data are:

1. The much wider range of melt compositions parental to the Troodos plutonics than is represented in the lavas demonstrates that the diverse melts generated within the melting column were much more poorly aggregated when they were added to the crust than by the time that their fractionated derivatives were erupted on the seafloor; i.e. melt aggregation occurred, to a large extent, within the crust.
2. The lower incompatible element abundances in the cores of cumulus clinopyroxene crystals from the Troodos plutonics than those from normal mid-ocean ridges indicate that the source region was significantly more depleted than the MORB source.
3. Vanadium systematics suggest the mantle source was initially depleted under relatively reducing conditions, such as at a normal mid-ocean ridge, followed by oxidation prior to, or during, extraction of the Troodos lavas.
4. Strontium (and LREE) enrichments with respect to clinopyroxene in gabbros from MORs indicate addition of a slab-derived component during melting.

That so much information can be gained from the trace element compositions of the cores of cumulus clinopyroxene crystals indicates that these could be very useful in investigating tectonic settings where basalts are unavailable.

Trace element characteristics of dykes cutting the Troodos plutonics

Dykes with chilled margins cutting the plutonic section provide evidence for the composition of melts formed after the melts parental to the plutonic section. The trace

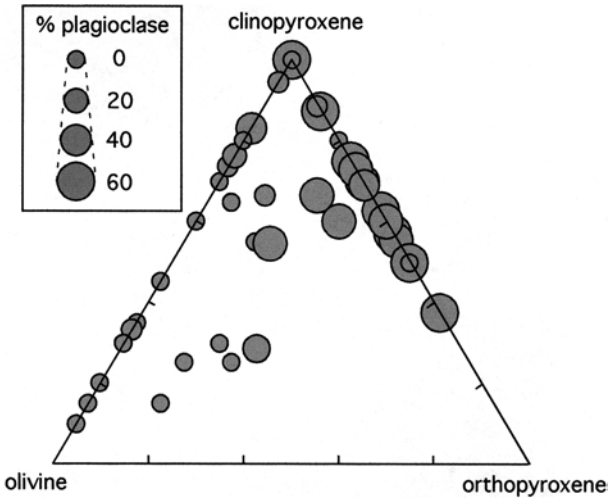

Fig. 2 Modal proportions of samples studied. Modes were estimated visually from thin sections. The plagioclase mode is proportional to the area of the symbol. The *key* shows representative sizes of *symbols* for different plagioclase modes

element compositions of six dykes that intrude the plutonic suite collected during this study are shown in Fig. 8, along with eight dykes cutting plutonic rocks from the Amiandos Area (Ash 1990). Most of these dykes show LREE and Nb enrichment with respect to middle-REE as well as positive Sr and Pb anomalies. A LREE-enrichment has been documented in some lavas from the western part of the Troodos complex (Taylor and Nesbitt 1988) as well as in, and to the south of, the Arakapas Fault Zone (e.g. McCulloch and Cameron 1983; Rogers et al. 1989). However, very depleted lava compositions (e.g. LREE <2x chondrite) have only been reported from south of the Arakapas Fault Zone. These depleted dykes are, however, in equilibrium with some of the depleted clinopyroxene analysed in this study (compare Figs. 6 and 8).

None of the dykes analysed in this study intrude highly depleted plutonic rocks. Their chilled margins and fine grain size do, however, suggest that they post-date all of the plutonic suite by a significant time interval. Two possible origins of these dykes are that they may represent a small volume off-axis magmatic event or they may record melts that were fed along axis from an offset spreading segment (possibly across the Arakapas Fault Zone). The orientations of dykes within the plutonic section are less systematic than in the overlying sheeted dyke complex (Table 7). This may either represent primary scatter in emplacement orientations or be due to rotations related to the uplift of Mt Olympus, which affect the plutonics more than the sheeted dyke complex.

Melt generation, extraction and aggregation beneath the Troodos spreading centre

The wide range of trace element abundances in the melts parental to the Troodos plutonics (Figs. 3, 5, 6 and 7) demonstrate that a broad range of melt compositions crossed the Moho. The compositional variability in these melts was much greater than that in erupted lavas, and ranged to much more depleted compositions (Fig. 7), indicating that a significant amount of the aggregation of the diverse melt compositions generated within the mantle occurred within the crust. This is despite the much smaller outcrop area of the plutonics than lavas, and the much greater number of studies that have addressed the lava compositions, suggesting that sampling biases cannot explain this observation. The small scale (hundreds of metres) over which large variations in trace element signatures exist within the plutonic section suggests that the melts

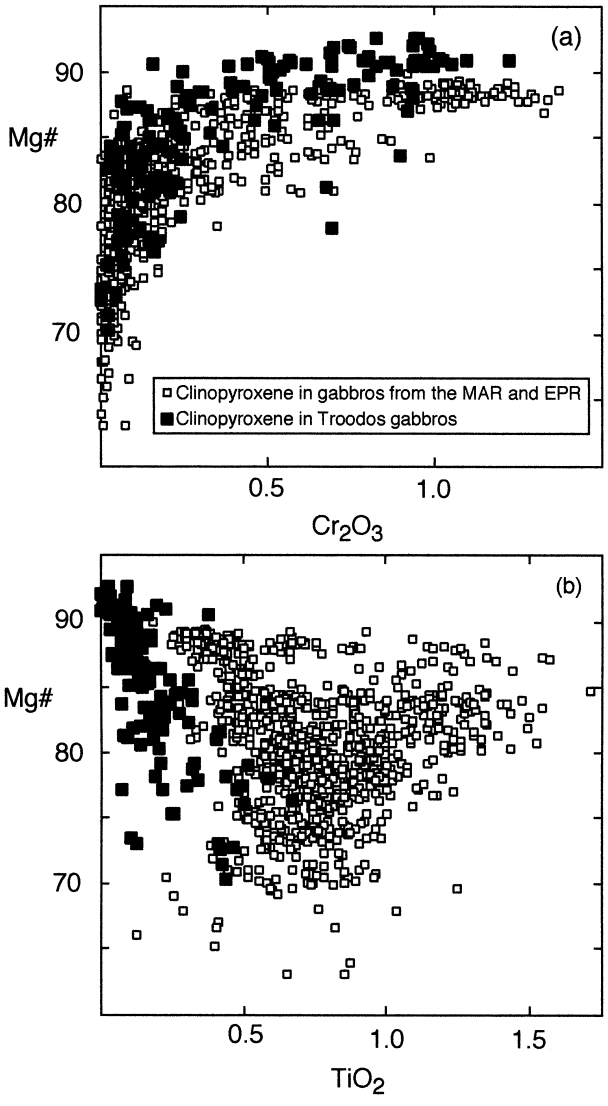

Fig. 3 A comparison of the major and minor element systematics of clinopyroxene in the Troodos plutonics and mid-ocean ridge gabbros (Coogan 1998; Coogan et al. 2002). Note the higher Mg# for a given Cr_2O_3 of the Troodos clinopyroxene which suggests a higher Mg# in the parental melt. Also, the lower TiO_2 at a given Mg# in the Troodos clinopyroxene indicates a more incompatible element depleted parental melt

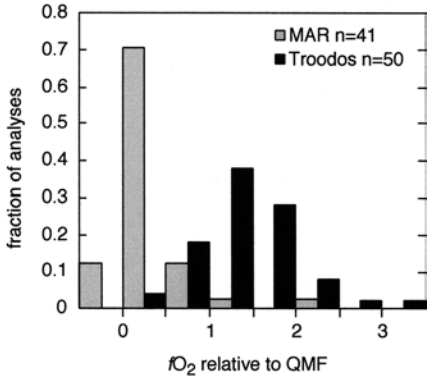

Fig. 4 Oxygen fugacity plotted relative to the quartz–magnetite–fayalite (*QMF*) buffer determined for the Troodos plutonics (data from this study; Thy 1987; Dunsworth 1989) and compared with plutonics from the Mid-Atlantic Ridge (*MAR*; Coogan 1998). The fO_2 determinations were made using the methodology of Sungawara (2001) assuming a pressure of 1.5 kbar and a temperature (1,045–1,145 °C) calculated from linear regression through experimental data for olivine forsterite content and temperature (Coogan 1998), although the exact temperature makes very little difference to the result. The average fO_2 of basaltic glasses from the MARK area of the MAR is 1.2 log units below QFM (Christie et al. 1986). See text for discussion

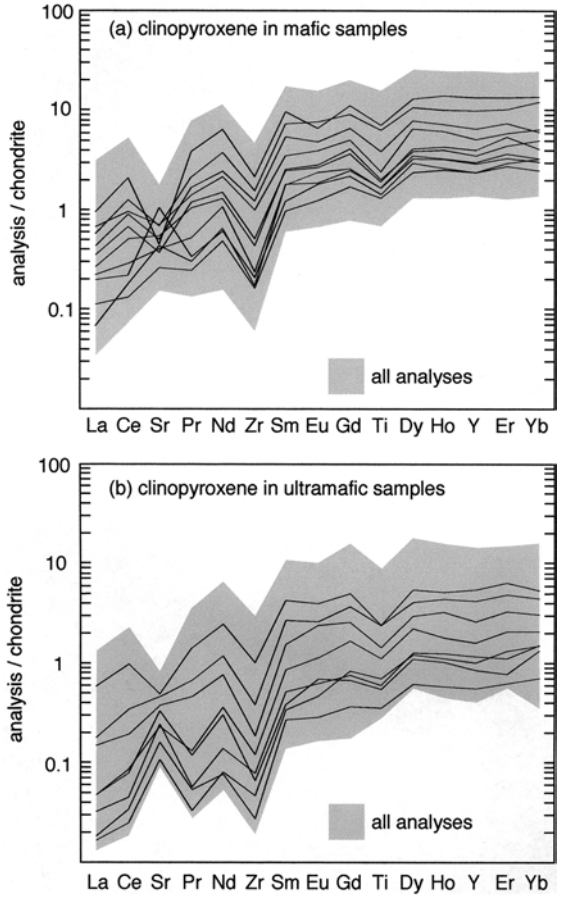

Fig. 5 Chondrite normalised (Anders and Grevesse 1989) spidergrams showing representative clinopyroxene analyses and fields of the entire dataset; **a** mafic samples; **b** ultramafic samples. Note the negative Zr anomalies and the variable (positive to negative) Sr anomalies

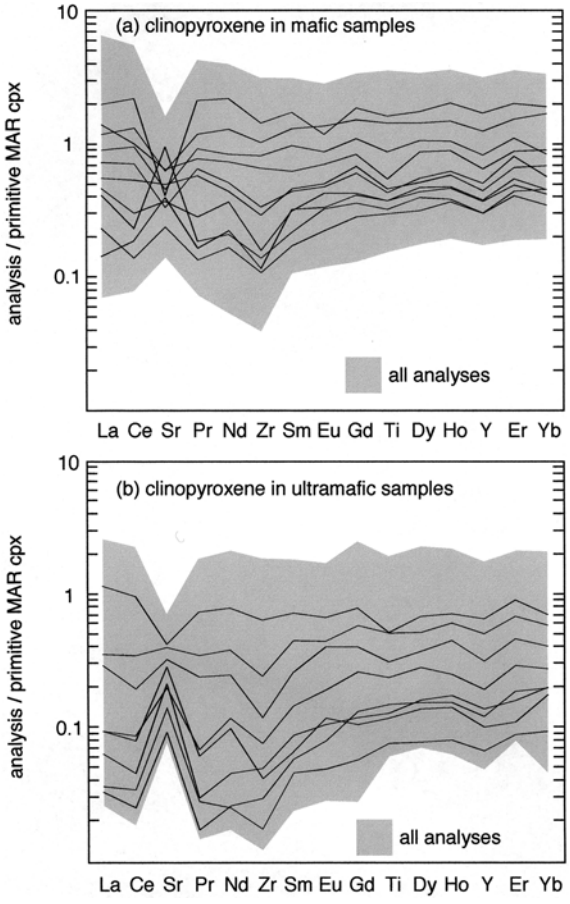

Fig. 6 Spidergrams showing the same analyses as in Fig. 5, but here normalised to the average (of seven analyses) composition of the most primitive clinopyroxene of Coogan et al. (2000a) from the MAR, which contains ~10,000 ppm Cr; **a** mafic samples; **b** ultramafic samples. Note (1) the generally lower incompatible element abundances, suggesting a parental melt with significantly lower incompatible element abundances than primitive MORB; (2) that the LREE are less depleted than expected considering the MREE and HREE depletion, and which in some cases are manifest in 'U-shaped' patterns; (3) positive Sr anomalies in many of the more depleted samples

added to the crust in any given place were quite variable. Crustal level magma plumbing, thus, did not aggregate all melts immediately they crossed the Moho because in this scenario their variability would not be preserved in the plutonic section. The compositional diversity was fairly efficiently mixed prior to eruption however, indicating that the crustal level magma plumbing effectively aggregated melts. Supplying the crust with highly variable, and generally depleted, melt compositions requires that melts are able to be extracted from the mantle without efficiently mixing with melts generated in other parts of the melting column. This suggests that the melts were extracted through conduits that tapped a limited volume of mantle and not through a perfect 'fractal tree' with efficient aggregation occurring within the mantle (Hart 1993).

It is clear that the Troodos lavas preserve much less of the compositional diversity generated within the

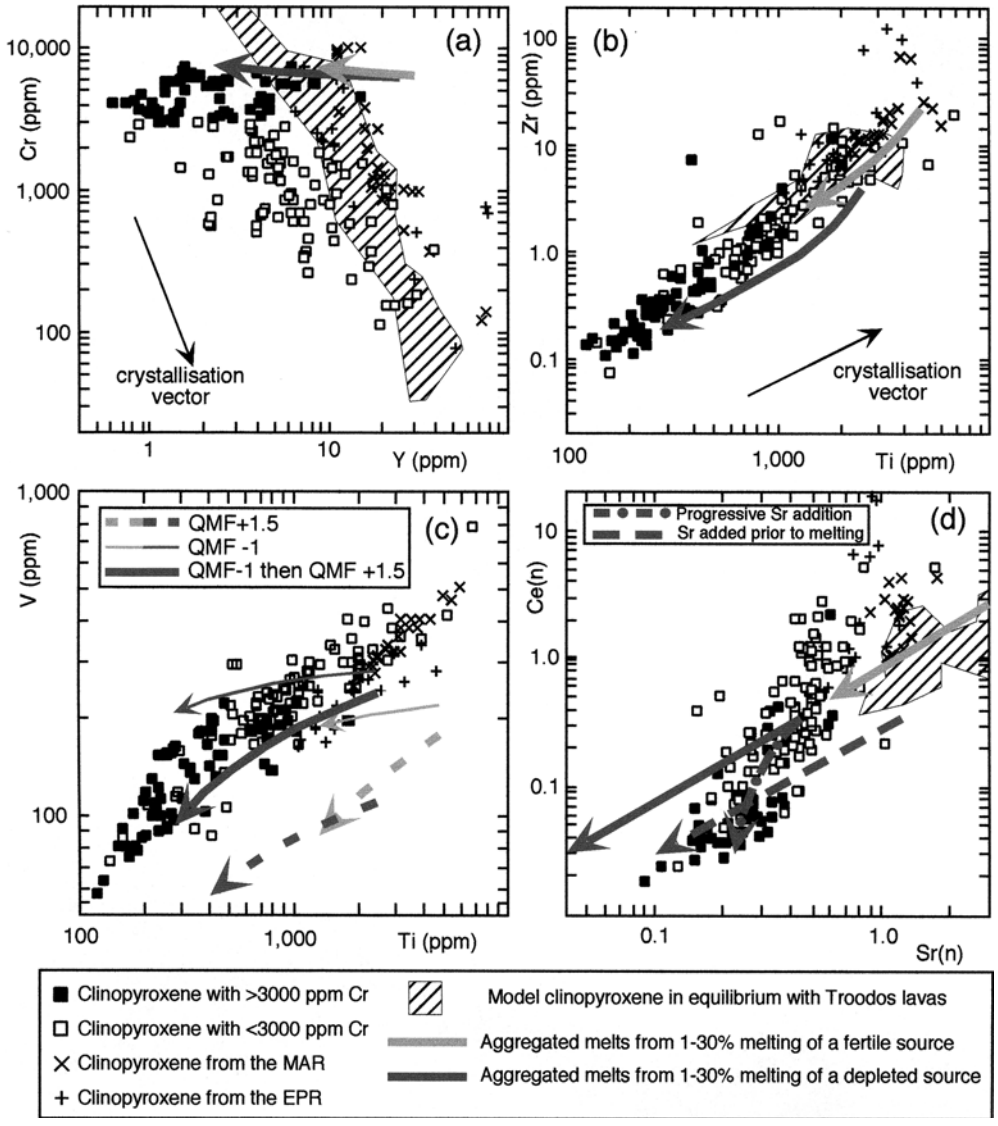

mantle than does the plutonic section. This has important implications for the use of lava geochemistry in interpreting mantle processes. Firstly, the continuous variation in clinopyroxene compositions demonstrate that a continuum of melt compositions were added to the crust, whereas several studies of lava chemistry have proposed the existence of multiple discrete compositions (e.g. McCulloch and Cameron 1983; Bednarz and Schmincke 1994). This implies that the diversity in lava compositions records an integrated signature that does not reflect the compositional diversity in individual melt batches added to the crust. Instead, it probably represents how these are pooled and fractionated within the crust prior to eruption. Secondly, the distribution of lava types does not necessarily reflect the distribution with which these different lava types are generated within the mantle. For example, highly depleted lavas with U-shaped spidergrams were apparently added to the entire Troodos crust (Fig. 6). In contrast, lavas with these compositions are only found in and to the south of the Arakapas Fault Zone and dykes with these compositions are only rare late features to the north of the Arakapas Fault Zone (Fig. 8). Using lava geochemistry, Murton (1989) and Rogers et al. (1989) suggest that these boninitic magmas were only generated in the mantle underlying the Arakapas Fault Zone and not in the main part of the Troodos massif due to the unusual tectonic environment. The data presented here lead to the alternative explanation that a much less robust lower crustal magma plumbing system in and to the south of the Arakapas Fault Zone simply allowed these melts to rise directly to the surface in this region, but not in the main part of the ophiolite, i.e. there is no requirement that different melt compositions were generated in the mantle beneath the Arakapas Fault Zone, instead, a different crustal magma plumbing system could simply have allowed the melts through to the surface with less mixing. The cross cutting dykes (Fig. 8) can be

◄

Fig. 7 Trace element characteristics of clinopyroxene in the Troodos plutonics: **a** Cr–Y showing the much lower Y, for a given Cr, of clinopyroxene in the Troodos plutonics in comparison with the cores of clinopyroxene crystals in plutonics from the MAR and East Pacific Rise (*EPR*). The smaller range of Y abundances in the more evolved (Cr-poor) clinopyroxenes than in the more primitive ones suggests that fractionation probably took place at the same time as mixing between magmas with different parental Y contents; **b** Ti–Zr showing the much lower abundances of these incompatible elements in clinopyroxene in plutonics from the Troodos ophiolite than the MAR and EPR; **c** V–Ti showing an offset of the Troodos clinopyroxene to higher V/Ti than clinopyroxene from the MAR and EPR. There is some uncertainty in the correct distribution coefficients to use for modelling V both because of its redox sensitivity and the importance of spinel in controlling the bulk distribution coefficient (e.g. Canil and Fedortchouk 2000). Despite this, it appears that the best explanation for the data is initial depletion of the Troodos mantle under reducing conditions, leading to a significant increase in the mantle V/Ti, followed by extraction of the Troodos parental melts under more oxidising conditions. The field of clinopyroxene in equilibrium with published Troodos lavas has been excluded for clarity and because of the uncertainties related to unknown oxygen fugacity and unknown quantities of oxide fractionation leading to V depletion. They lie in the region V: 30–160 ppm (QFM + 1.5) or 90–600 ppm (QFM-1) and Ti: 400–3600 ppm; **d** $Ce_{(n)}$–$Sr_{(n)}$, where $_{(n)}$ denotes chondrite normalised using the values of Anders and Grevesse (1989) showing that Sr is not depleted as rapidly as Ce. Furthermore, the suprachondritic Sr/Ce of many samples indicates addition of Sr with respect to Ce presumably from the slab. This can be modelled by progressive addition of Sr to the source during melting. In the incremental melting model shown, 0.02× chondrite Sr was added to the depleted source after each 1% melting. The absolute concentration of Sr required to fit the data depends on the starting compositions and whether any Ce is also added during melting; thus, the modelling is schematic and is not intended to quantify the amount of Sr added. Addition of Sr to the source prior to melting cannot reproduce the data as shown. The melting models show the composition of clinopyroxene in equilibrium with the aggregated melts produced by 0 to 30% fractional melting using the source compositions and distribution coefficients given in Table 6. Of course, in reality neither the source composition nor the distribution coefficients would be constant and it is likely that, if the source was depleted at a normal mid-ocean ridge, its composition would be vertically stratified. Also, small amounts of olivine crystallisation prior to clinopyroxene saturation could increase the concentrations of all elements within the melt, but this effect is insignificant compare with uncertainty in distribution coefficients and source compositions. Crystallisation trends are schematic, but crystallisation can be assumed to have had little effect on the incompatible trace element composition of clinopyroxene containing > 3,000 ppm Cr. The field of clinopyroxene in equilibrium with published lava compositions is calculated using the distribution coefficients in Table 6 from the lava data presented by Rautenschlein et al. (1985), Cameron (1985), Taylor (1990), Sobolev et al. (1993), Bednarz and Schmincke (1994) and Gillis (unpublished) for lavas from north of the Arakapas Fault Zone. No lavas from south of the Arakapas Fault Zone are included as all the plutonics studied come from north of this fault and because this area has previously been suggested to have been compositionally distinct (e.g. Murton 1989). Because of the paucity of Zr and Y data, the abundances of these were estimated from Hf and HREE abundances in some instances assuming chondritic Zr/Hf and Y/HREE ratios

interpreted in the same way, either forming 'off-axis' where much less magma was generated reducing the chances of mixing, or being fed from within or south of the Arakapas Fault Zone. Thus, the lack of boninites in volcanic sequences does not necessarily mean that boninitic melts were not generated and even added to the crust. It also indicates that the spatial distribution of depleted lava-types does not have to 'map-out' the locations where these magma-types are generated, but simply where they are able to traverse the crust without mixing with, or assimilating, less depleted magmas/rock.

An important questions is how representative of a normal mid-ocean ridge was the magma plumbing system beneath the Troodos ophiolite? Unlike at normal mid-ocean ridges melting beneath the Troodos ophiolite was, at least in part, due to the addition of a H_2O-bearing subduction component. Primitive melt inclusions trapped in olivine phenocrysts in the Troodos lavas contain 1.36–2.12 wt% H_2O (Sobolev and Chaussidon 1996). Modelling using the thermodynamically based software pMELTS (Ghiorso and Hirschmann 1998) indicates that isobaric addition of 0.2 wt% H_2O to a depleted mantle composition (from Kinzler and Grove 1992) at its dry solidus, under equilibrium conditions, can produce ~10% melt containing ~2 wt% H_2O (i.e. similar to the Troodos parental melts). A similarly large increase in melt fraction due to H_2O addition is predicted by the experiments of Gaetani and Grove (1998). The thin Troodos crust (≤ 5 km) could thus be generated almost entirely through flux melting of the mantle with relatively little decompressional melting. This is consistent with the Troodos ophiolite forming during subduction initiation when mantle previously depleted at a normal mid-ocean ridge flows into the 'proto-wedge' generated by the initiation of subduction. At this stage, the mantle flow would have a large horizontal component (e.g. Fig. 6 of Stern and Bloomer 1992). This line of reasoning raises the possibility that the Troodos magma plumbing system could have been quite different from that at normal mid-ocean ridges. For example, (1) the melting region may have been defined by where addition of slab components led to melting and not by the region of adiabatically decompressing mantle, (2) the mantle viscosity is likely to have been much lower than that at a mid-ocean ridge due to the effect of H_2O on rheology (Hirth and Kohlstedt 1996; Billen and Gurnis 2001) and (3) the existence of a subsiding or subducting slab may have limited the maximum depth of melt generation and influenced mantle flow. Both a low mantle viscosity and only limited upwelling may lead to much less well-organised melt extraction than at mid-ocean ridges. In particular, if melt focusing to the neovolcanic zone at mid-ocean ridges is influenced by the pressure gradient induced by corner flow (Spiegelman and McKenzie 1987) then the low viscosity, and limited upwelling leading to limited corner flow, will have led to much less well focused melt extraction (e.g. Hirth and Kohlstedt 1996). Poorly focused melt extraction is consistent with the extraction of a large range of melt compositions from the mantle into the lower crust as suggested by the compositions of the cores of cumulus clinopyroxene crystals in the plutonics (Figs. 6

Table 6 Starting compositions and distribution coefficients used in the modelling in Fig. 7

	Distribution coefficient			Starting composition	
	Fertile source	Depleted source	Clinopyroxene	Fertile source	Depleted source
Cr	4.01[a]	4.31[b]	10[c]	2,340[d]	2,650[e]
Y	0.09[a]	0.02[b]	0.7[c]	4[d]	1.0[e]
Ti	0.08[a]	0.03[b]	0.4[c]	1,020[d]	216[e]
Zr	0.03[a]	0.01[b]	0.12[f]	7[d]	0.5[e]
V QFM-1	0.50[g]	0.34[g]	1.47[g]	73[d]	63[e]
V QFM + 1.5	0.16[g]	0.12[g]	0.39[g]	73[d]	34[e]
Sr(n)	0.025[h]	0.02[h]	0.1[i]	1.67[d]	0.11[e]
Ce(n)	0.025[h]	0.02[h]	0.1[i]	1.38[d]	0.09[e]

[a]Pearce and Parkinson (1993; their spinel lherzolite at 1,300 °C). Based on data in Duke (1976), Dupuy et al. (1980), Hervig et al. (1986) and Stosch (1981)
[b]Pearce and Parkinson (1993; their harzburgite at 1,300 °C)
[c]Pearce and Parkinson (1993; clinopyroxene at 1,200 °C)
[d]Frey et al. (1985) sample 717
[e]Calculated as the residue of 15% fractional melting mixed with 1% aggregated melt to account for incomplete melt extraction
[f]Hart and Dunn (1993)
[g]Calculated from the distribution coefficient data of Canil and Fedortchouk (2000) for modes of 55% olivine, 1.5% spinel, 13.5% clinopyroxene and 29% orthopyroxene for the fertile source and 63% olivine, 1% spinel, 7% clinopyroxene and 28% orthopyroxene in the depleted source with 1% porosity
[h]Calculated from modes given in ([g]) and distribution coefficients from Hart and Dunn (1993); Beattie (1993, 1994) and Schwandt and McKay (1998)
[i]Average of numerous published values (e.g. Hart and Dunn 1993; Jenner et al. 1994)

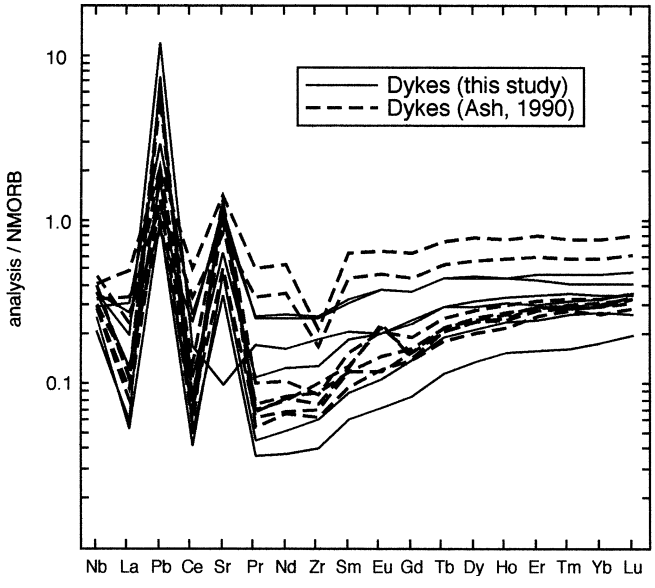

Fig. 8 NMORB (Sun and McDonough 1989) normalised spidergrams of dykes intruding the plutonics. *Solid lines* This study; *dashed lines* Ash (1990). A notable characteristic of these dykes is the small variation in Nb abundances despite the large variation in LREE abundances, which leads to positive Nb anomalies in the more depleted dykes

and 7). Thus, it is possible that the magma plumbing system beneath the Troodos (and other?) ophiolite differed in several ways from that at normal mid-ocean ridges.

Summary and conclusions

Trace element analyses of the cores of cumulus clinopyroxene crystals indicate that the range of melt compositions added to the lower crust during the formation of the Troodos ophiolite far exceeded that erupted on the seafloor. This crustal level aggregation and concomitant fractionation was important in controlling the compositions erupted. Much more depleted melts, with LREE and Sr enrichments, were added to the crust than were erupted on the seafloor. Thus, the distribution of lava types does not necessarily record where different magma types are generated, but simply where they are able to traverse the magma plumbing system with limited interaction with other magma types.

In comparison to clinopyroxene crystals in the cumulates formed from normal mid-ocean ridge basalts the Troodos cumulus clinopyroxene are (1) generally depleted in incompatible trace elements, (2) less depleted in LREE than would be expected for the concomitant depletion in HREE and (3) enriched in Sr with respect to the LREE. Furthermore, the partitioning of iron between plagioclase and olivine indicates the parental magmas for the Troodos ophiolite were more oxidised than MORB. These characteristics are similar to those that can be identified using fresh basalts, indicating that there is significant promise in using clinopyroxene trace element systematics (± plagioclase–olivine oxygen barometry) as a fingerprint of parental melt composition and thus, potentially, a tectonic setting.

Table 7 Whole-rock trace element (ppm) compositions of dykes cutting the plutonic complex

Orientation	99CL3 210/28°NW	99CL21 080/72°N	99CL38 070/75°SE	99CL46 095/65°N	99CL51 135/75°NE	99CL71 185/85°E
Sr	87.6	8.7	42.3	31.2	56.2	103.2
Y	11.63	8.67	5.85	3.82	7.91	10.20
Zr	19.16	13.92	4.43	3.01	9.48	18.39
Nb	0.68	0.83	0.58	0.49	0.83	0.83
La	0.78	0.49	0.13	0.15	0.32	0.68
Ce	1.96	1.24	0.31	0.37	0.81	1.77
Pr	0.34	0.23	0.06	0.05	0.14	0.33
Nd	1.93	1.21	0.38	0.27	0.92	1.85
Sm	0.87	0.54	0.23	0.16	0.49	0.82
Eu	0.38	0.21	0.11	0.07	0.20	0.38
Gd	1.34	0.89	0.51	0.30	0.84	1.34
Tb	0.29	0.20	0.13	0.08	0.20	0.29
Dy	2.07	1.35	0.96	0.62	1.45	1.98
Ho	0.45	0.31	0.24	0.15	0.34	0.44
Er	1.40	0.91	0.72	0.48	1.03	1.29
Tm	0.21	0.15	0.12	0.07	0.16	0.18
Yb	1.40	1.01	0.82	0.54	1.05	1.25
Lu	0.22	0.16	0.12	0.09	0.16	0.19
Pb	0.86	3.57	0.29	2.19	0.50	0.25

Acknowledgments We would like to express our gratitude to Richard Hinton and John Craven for their expert help during SIMS analysis, Rob Wilson for his support during electron probe analysis and Sarah Goldsmith for her assistance during ICP-MS analysis. Discussions with Craig Manning during the initial fieldwork, the leaders and participants in the RIDGE and INTERIDGE summer schools in Cyprus in 1999, and Steve Edwards were helpful, as were discussion with Hans Schouten regarding his models for upper crustal accretion and Dante Canil about V partitioning. Two anonymous journal reviewer are thanked for their constructive criticism and Tim Grove is thanked for editorial handling. Informal reviews from Mike O'Hara, Andrew Kerr and Richard Thomas helped to improve the manuscript. SIMS analyses were funded through Natural Environment Research Council grant IMP 149/1099.

References

Anders E, Grevesse N (1989) Abundances of the elements: meteoric and solar. Geochim Cosmochim Acta 53:197–214

Ash CH (1990) Development and subsequent demise of an oceanic spreading center: the Troodos ophiolite, Cyprus. MSc Thesis, Memorial University of Newfoundland

Baragar WRA, Lambert MB, Baglow N, Gibson I (1987) Sheeted dykes of the Troodos ophiolite, Cyprus. In: Hall HC, Fahrig WF (eds) Mafic dyke swarms. Geological Association of Canada Special Paper, pp 257–272

Beattie P (1993) The generation of uranium series disequilibria by partial melting of spinel peridotite: constraints from partitioning studies. Earth Planet Sci Lett 117:379–391

Beattie P (1994) Systematics and energetics of trace-element partitioning between olivine and silicate melts: implications for the nature of mineral/melt partitioning. Chem Geol 117:57–71

Bednarz U, Schmincke H-U (1994) Petrological and chemical evolution of the northeastern Troodos extrusive series, Cyprus. J Petrol 35:489–523

Benn K (1986) Petrology of the Troodos plutonic complex in the Caledonian Falls area, Cyprus. MSc Thesis, Université Laval, Quebec

Benn K, Laurent R (1987) Intrusive suite documented in the Troodos ophiolite plutonic complex, Cyprus. Geology 15:821–824

Billen MI, Gurnis M (2001) A low viscosity wedge in subduction zones. Earth Planet Sci Lett 193:227–236

Browning P, Roberts S, Alabaster T (1989) Fine scale modal layering and cyclic units in ultramafic cumulates from the CY-4 borehole, Troodos ophiolite: evidence for an open system magma chamber. In: Gibson IL, Malpas J, Robinson PT, Xenophontos C (eds) Cyprus crustal study project. Initial report, Hole CY-4, Geological Survey of Canada report 88-9, pp 193–220

Cameron WE (1985) Petrology and origin of primitive lavas from the Troodos ophiolite, Cyprus. Contrib Mineral Petrol 89:239–255

Canil D (1999) Vanadium partitioning between orthopyroxene, spinel and silicate melt and the redox states of mantle source regions for primary magmas. Geochim Cosmochim Acta 63:557–572

Canil D, Fedortchouk Y (2000) Clinopyroxene–liquid partitioning for vanadium and the oxygen fugacity during formation of cratonic and oceanic mantle lithosphere. J Geophys Res 105:26003–26016

Cannat M (1991) Plastic deformation at an oceanic spreading ridge: a microstructural study of the Site 735 gabbros (Southwest Indian Ridge). In: Von Herzen PR, Robinson PT (eds) Proceedings of the Ocean Drilling Program Leg 118, scientific results. US Government Printing Office, Washington, DC, pp 399–408

Christie DM, Carmichael ISE, Langmuir CH (1986) Oxidation states of mid-ocean ridge basalt glasses. Earth Planet Sci Lett 79:397–411

Coogan LA (1998) Magma plumbing beneath the Mid-Atlantic Ridge. PhD Thesis, Leicester University

Coogan LA, Kempton PD, Saunders AD, Norry MJ (2000a) Evidence from plagioclase and clinopyroxene major and trace element compositions for melt aggregation within the crust beneath the Mid-Atlantic Ridge. Earth Planet Sci Lett 176:245–257

Coogan LA, Saunders AD, Kempton PD, Norry MJ (2000b) Evidence from oceanic gabbros for porous melt migration within a crystal mush beneath the Mid-Atlantic Ridge. Geochemistry, Geophysics, Geosystems, vol 1, paper no 2000GC000072

Coogan LA, Gillis KM, MacLeod CJ, Thompson G, Hekinian R (2002) Petrology and geochemistry of the lower ocean crust formed at the East Pacific Rise and exposed at Hess Deep: a synthesis and new results. Geochemistry, Geophysics, Geosystems (in press)

Duke JM (1976) Distribution of period four transition elements amongst olivine, calcic clinopyroxene and mafic silicate liquid: experimental results. J Petrol 17:499–521

Dunsworth SM (1989) Multiple intrusion and deformation within the northwestern quadrant of the plutonic complex, Troodos ophiolite, Cyprus. MSc Thesis, Memorial University of Newfoundland

Dupuy C, Dostal J, Liotard JM, Leyreloup A (1980) Partitioning of transition elements between clinopyroxene and garnet. Earth Planet Sci Lett 48:303–310

Frey FA, Suen J, Stockman HW (1985) The Ronda high temperature peridotite: geochemistry and petrogenesis. Geochim Cosmochim Acta 49:2469–2491

Gaetani GA, Grove TL (1995) Partitioning of rare-earth elements between clinopyroxene and silicate melt: crystal-chemical controls. Geochim Cosmochim Acta 59:1951–1962

Gaetani GA, Grove TL (1998) The influence of water on melting of mantle peridotite. Contrib Mineral Petrol 131:323–346

Geological Survey Department Cyprus (1995) Geological map of Cyprus. Ministry of Agriculture, Natural Resources and Environment, Cyprus

Ghiorso MS, Hirschmann MM (1998) pMELTS: a revised calibration of MELTS for modelling peridotite melting at high pressure. EOS Trans 79(45):F1005

Hart SR (1993) Equilibration during mantle melting: a fractal tree model. Proc Natl Acad Sci USA 90:11914–11918

Hart SR, Dunn T (1993) Experimental cpx/melt partitioning of 24 trace elements. Contrib Mineral Petrol 113:1–8

Hervig RL, Smith JV, Dawson JB (1986) Lherzolite xenoliths in kimberlites and basalts: petrogenetic and crystallographic significance of some minor and trace elements in olivine, pyroxenes, garnet and spinel. Trans R Soc 77:181–201

Hirth G, Kholstedt DL (1996) Water in the oceanic upper mantle: implications for rheology, melt extraction and the evolution of the lithosphere. Earth Planet Sci Lett 144:93–108

Jenner GA, Foley SF, Jackson SE, Green TH, Fryer BJ, Longerich HP (1994) Determination of partition coefficients for trace elements in high pressure–temperature experimental run products by laser ablation microprobe-inductively coupled plasma-mass spectrometry. Geochim Cosmochim Acta 58:5099–5103

Johnson KTM, Dick HJB, Shimizu N (1990) Melting in the oceanic upper mantle: an ion-microprobe study of diopsides in abyssal peridotites. J Geophys Res 95:2661–2678

Kinzler RJ, Grove TL (1992) Primary magmas of mid-ocean ridge basalts. 2. Applications. J Geophys Res 97:6907–6926

Klein EM, Langmuir CH (1987) Global correlation of ocean ridge basalt chemistry with axial depth and crustal thickness. J Geophys Res 92:8089–8115

MacLeod CM (1990) Role of the southern Troodos Transform in the rotation of the Cyprus microplate: evidence from the eastern Limassol Forest Complex. In: Malpas J, Moores EM, Panayiotou A, Xenophontos C (eds) Ophiolites – oceanic crustal analogues. Geological Survey Department, Ministry of Agriculture and Natural Resources, Cyprus, pp 75–85

Malpas J (1990) Crustal accretionary processes in the Troodos ophiolite, Cyprus: evidence from field mapping and deep crustal drilling. In: Malpas J, Moores EM, Panayiotou A, Xenophontos C (eds) Ophiolites – oceanic crustal analogues. Geological Survey Department, Ministry of Agriculture and Natural Resources, Cyprus, pp 65–74

Malpas J, Brace T (1987) The geology of Pano Amiandos – Palekhori area, Cyprus (map). Geological Survey Department, Cyprus

Malpas J, Case G, Moore P (1989) The geology of the area immediately surrounding the CY-4 borehole of the Cyprus Crustal Study Project. In: Gibson IL, Malpas J, Robinson PT, Xenophontos C (eds) Cyprus crustal study project. Initial report, Hole CY-4, Geological Survey of Canada report 88-9, pp 31–37

McBirney AR, Nicolas A (1997) The Skaergaard layered series. Part II. Magmatic flow and dynamic layering. J Petrol 38:569–580

McCulloch MT, Cameron WE (1983) Nd–Sr isotopic study of primitive lavas from the Troodos ophiolite, Cyprus: evidence for a subduction-related setting. Geology 11:727–731

Miyashiro A (1973) The Troodos ophiolite was probably formed in an island arc. Earth Planet Sci Lett 19:218–224

Mukasa SB, Ludden JN (1987) Uranium–lead isotopic ages of plagiogranites from the Troodos ophiolite, Cyprus, and their tectonic significance. Geology 15:825–828

Murton BJ (1989) Tectonic controls on boninite genesis. In: Saunders AD, Norry MJ (eds) Magmatism in the ocean basins. Geol Soc Lond Spec Publ 42:347–377

Panjasawatwong Y, Danyushevsky LV, Crawford AJ, Harris KL (1995) An experimental study of the effects of melt composition on plagioclase–melt equilibria at 5 and 10 kbars: implications for the origin of magmatic high An plagioclase. Contrib Mineral Petrol 118:420–432

Parkinson IJ, Arculus RJ (1999) The redox state of subduction zones: insights from arc-peridotites. Chem Geol 160:409–423

Pearce JA, Parkinson IJ (1993) Trace element models for mantle melting: application to volcanic arc petrogenesis. In: Prichard HM, Alabaster T, Harris NBW, Neary CR (eds) Magmatic processes and plate tectonics. Geol Soc Lond Spec Publ 76:373–403

Pearce JA, Lippard SJ, Roberts S (1984) Characteristics and tectonic significance of supra-subduction zone ophiolites. Geol Soc Lond Spec Publ 16:77–94

Pearce NJG, Perkins WT, Westgate JA, Gorton MP, Jackson SE, Neal CR, Chenery SP (1997) A compilation of new and published major and trace element data for NIST SRM 610 and NIST SRM 612 glass reference materials. Geostand Newsl 21:115–144

Phinney WC (1992) Partition coefficients for iron between plagioclase and basalt as a function of oxygen fugacity: implications for Archean and lunar anorthosites. Geochim Cosmochim Acta 56:1885–1895

Portnyagin MV, Danyushevsky LV, Kamenetsky VS (1997) Coexistence of two distinct mantle sources during the formation of ophiolites: a case study of primitive pillow-lavas from the lowest part of the volcanic section of the Troodos Ophiolite, Cyprus. Contrib Mineral Petrol 128: 287–301

Rautenschlein M, Jenner GA, Hertogen J, Hofmann AW, Kerrich R, Schmincke H-U, White WM (1985) Isotopic and trace element composition of volcanic glasses from the Akaki Canyon, Cyprus: implications for the origin of the Troodos ophiolite. Earth Planet Sci Lett 75:369–383

Robertson AHF (1990) Tectonic evolution of Cyprus. In: Malpas J, Moores EM, Panayiotou A, Xenophontos C (eds) Ophiolites – oceanic crustal analogues. Geological Survey Department, Ministry of Agriculture and Natural Resources, Cyprus, pp 235–252

Robinson PT, Melson WG, O'Hearn T, Schmincke H-U (1983) Volcanic glass compositions of the Troodos ophiolite, Cyprus. Geology 11:400–404

Rogers NW, MacLeod CJ, Murton BJ (1989) Petrogenesis of boninitic lavas from the Limassol Forest Complex, Cyprus. In: Crawford AJ (ed) Boninites, Unwin, pp 288–313

Schouten H, Denham CR (2000) Comparison of volcanic construction in the Troodos ophiolite and oceanic crust using paleomagnetic inclinations from Cyprus Crustal Study Project (CCSP) CY-1 and CY-1A and Ocean Drilling Program (ODP) Hole 504B drill cores. In: Dilek Y, Moores E, Elthon D, Nicolas A (eds) Ophiolites and ocean crust. Geol Soc Am Spec Pap 349:181–194

Schwandt CS, McKay GA (1998) Rare earth element partition coefficients from enstatite/melt synthesis experiments. Geochim Cosmochim Acta 62:2845–2848

Shervais JW (1982) Ti–V plots and the petrogenesis of modern and ophiolitic lavas. Earth Planet Sci Lett 59:101–118

Shimizu N (1981) Trace element incorporation into growing augite phenocryst. Nature 289:575–577

Sneeringer M, Hart SR, Shimizu N (1984) Strontium and samarium diffusion in diopside. Geochim Cosmochim Acta 48:1589–1608

Sobolev AV, Chaussidon M (1996) H_2O concentrations in primary melts from supra-subduction zones and mid-ocean ridges: implications for H_2O storage and recycling in the mantle. Earth Planet Sci Lett 137:45–55

Sobolev AV, Shimizu N (1993) Ultra-depleted primary melt inclusions in an olivine from the Mid-Atlantic Ridge. Nature 363:151–154

Sobolev AV, Portnyagin MV, Dmitriev LV, Tsameryan OP, Danyushevsky LV, Kononkova NN, Shimizu N, Robinson PT (1993) Petrology of ultramafic lavas and associated rocks of the Troodos Massif, Cyprus. Petrology 1:379–412

Sours-Page R, Johnson KTM, Nielsen RL, Karsten JL (1999) Local and regional variation in MORB parental magmas: evidence from melt inclusions from the Endeavor Segment of the Juan de Fuca Ridge. Contrib Mineral Petrol 134:342–363

Spiegelman M, McKenzie D (1987) Simple 2-D models for melt extraction at mid-ocean ridges and island arcs. Earth Planet Sci Lett 83:137–152

Stern RJ, Bloomer SH (1992) Subduction zone infancy: examples from the Eocene Izu–Bonin–Mariana and Jurassic California arcs. Geol Soc Am Bull 104:1621–1636

Stosch H-G (1981) Sc, Cr, Co and Ni partitioning between minerals from spinel peridotite xenoliths. Contrib Mineral Petrol 78: 166–174

Sun S-S, McDonough WF (1989) Chemical and isotopic systematics of oceanic basalts: implications for mantle composition and processes. In: Saunders AD, Norry MJ (eds) Magmatism in the ocean basins. Geol Soc Lond Spec Publ 42:313–345

Sungawara T (2001) Ferric iron partitioning between plagioclase and silicate liquid: thermodynamics and petrological applications. Contrib Mineral Petrol 141:659–686

Taylor RN (1990) Geochemical stratigraphy of the Troodos extrusive sequence: temporal developments of a spreading center magma chamber. In: Malpas J, Moores EM, Panayiotou A, Xenophontos C (eds) Ophiolites – oceanic crustal analogues. Geological Survey Department, Ministry of Agriculture and Natural Resources, Cyprus, pp 173–183

Taylor RN, Nebitt RW (1988) Light rare-earth enrichment of supra subduction zone mantle: evidence from the Troodos ophiolite, Cyprus. Geology 16:448–451

Thy P (1987) Magmas and magma chamber evolution, Troodos ophiolite, Cyprus. Geology 15:316–319

Thy P, Moores EM (1988) Crustal accretion and tectonic setting of the Troodos ophiolite, Cyprus. Tectonophysics 147:221–245

Thy P, Xenophontos C (1991) Crystallization orders and phase chemistry of glassy lavas from the pillow sequences, Troodos Ophiolite, Cyprus. J Petrol 32:403–428

Van Orman JA, Grove TL, Shimizu N (2001) Rare earth element diffusion in diopside: influence of temperature, pressure, and ionic radius and an elastic model for diffusion in silicates. Contrib Mineral Petrol 141:687–703

Vine FJ, Smith GC (1990) Structure and physical properties of the Troodos crustal section at ICRDG drillholes CY1, 1a and 4. In: Malpas J, Moores EM, Panayiotou A, Xenophontos C (eds) Ophiolites – oceanic crustal analogues. Geological Survey Department, Ministry of Agriculture and Natural Resources, Cyprus, pp 113–124

Watson EB (1996) Surface enrichment and trace-element uptake during crystal growth. Geochim Cosmochim Acta 60: 5013–5060

Wilson RAM (1959) The geology of the Xeros–Troodos area. Geological Survey Department Cyprus, Memoir 1, Department Ministry of Agriculture and Natural Resources

Wood BJ, Blundy JD (1997) A predictive model for rare earth element partitioning between clinopyroxene and anhydrous silicate melt. Contrib Mineral Petrol 129:166–181